6 EXTRA GAUGE GROUPS

6.1 Introduction

Paul Langacker, Alexei Raspereza and Sabine Riemann

6.1.1 Classes of models

Extended gauge symmetries and/or extra gauge bosons appear in many extensions of the standard model, such as left-right symmetric models [1], superstring motivated models [2], GUT (grand unification theory) [3], little Higgs models [4], large extra dimensions [5], and dynamical symmetry breaking [6]. In many cases, the extra symmetry is broken at the TeV scale, leading not only to additional gauge bosons, but also to an extended Higgs sector (needed to break the gauge symmetry), extended neutralino/chargino sectors [7, 8] (with implications for dark matter), new sources of CP violation at tree level in the Higgs sector [9, 10] (important for collider physics and baryogenesis), new fermions [11] (for anomaly cancellation), new sources of Higgs [12] or Z' [13]-mediated flavor-changing neutral currents, and new constraints or parameter ranges for the Standard Model (SM) or MSSM. Here, we focus on the additional Higgs bosons, which may dramatically affect the Higgs collider signatures, taking the cases of $SU(2)_L \times U(1)_Y \times U(1)'$ [3] and left-right symmetric $SU(2)_L \times SU(2)_R \times U(1)_{B-L}$ [1] for definiteness.

Especially common are new $U(1)'$ gauge symmetries, broken by the expectation values of standard model singlets S. In most supersymmetric examples, the $U(1)'$ symmetry forbids elementary μ terms, but may allow trilinear superpotential couplings

$$W = h_s S H_u H_d. \tag{6.1}$$

If S acquires a vacuum expectation value $\langle S \rangle$, an effective μ parameter $\mu_{eff} = h_s \langle S \rangle$ is generated. This is in the needed range for $h_s < O(0.8)$ (needed if h_s is to remain perturbative up to the Planck scale) and $\langle S \rangle$ is in the 100 GeV-1 TeV range (expected if the $U(1)'$ and electroweak scales are both set by the scale of soft supersymmetry breaking). In this respect, the $U(1)'$ models are similar to the NMSSM and related models. However, there are no discrete symmetries and therefore no danger of cosmological domain walls.

The simplest class of models involve a single S field. Then, the potential for S and the neutral components of $H_{u,d}$ is given by

$$V = V_F + V_D + V_{soft}, \tag{6.2}$$

where

$$V_F = h_s^2 \left(|H_d|^2 |H_u|^2 + |S|^2 |H_d|^2 + |S|^2 |H_u|^2 \right), \tag{6.3}$$

$$V_D = \frac{g_1^2 + g_2^2}{8} \left(|H_u|^2 - |H_d|^2 \right)^2 + \frac{1}{2} g_{Z'}^2 \left(Q_S |S|^2 + Q_{H_d} |H_d|^2 + Q_{H_u} |H_u|^2 \right)^2, \tag{6.4}$$

and

$$V_{soft} = m_{H_d}^2 |H_d|^2 + m_{H_u}^2 |H_u|^2 + m_S^2 |S|^2 - (A_h h_s S H_d H_u + \text{H.C.}), \tag{6.5}$$

where g_1, g_2, and $g_{Z'}$ are respectively the $U(1)$, $SU(2)$, and $U(1)'$ gauge couplings, and Q_i is the $U(1)'$ charge of particle i. Of course, the coupling (6.1) requires that $Q_S + Q_{H_d} + Q_{H_u} = 0$. The last ($A_h$) term in V_{soft} is the analog of the $B\mu$ term of the MSSM. (The MSSM limit of the model is obtained for $h_s \to 0$ with μ_{eff} held fixed.)

The spectrum of physical Higgses after symmetry breaking [14–26] consists of three neutral CP even scalars (h_i^0, $i = 1, 2, 3$), one CP odd pseudoscalar (A^0) and a pair of charged Higgses ($H^\pm$), i.e., it has one scalar more than in the MSSM. Masses for the three neutral scalars are obtained by diagonalizing the corresponding 3×3 mass matrix. The tree level mass of the lightest scalar h_1^0 satisfies the bound

$$m_{h_1^0}^2 \leq M_Z^2 \cos^2 2\beta + \frac{1}{2} h_s^2 v^2 \sin^2 2\beta + g'^2 \overline{Q}_H^2 v^2, \tag{6.6}$$

where $\overline{Q}_H = \cos^2\beta Q_1 + \sin^2\beta Q_2$; $v^2 \equiv v_1^2 + v_2^2 \sim (246\ \mathrm{GeV})^2$, where $v_i \equiv \sqrt{2}\langle H_i^0\rangle$; and $\tan\beta \equiv v_2/v_1$. In contrast to the MSSM, h_1^0 can be heavier than M_Z at tree level, both due to the F-term contributions (similar to the NMSSM) and the D-terms. Including the radiative corrections (which are similar to the MSSM), the MSSM upper bound of ~ 130 GeV can be relaxed to $O(170)$ GeV.

The Higgs spectrum is particularly simple in the large $s \equiv \sqrt{2}\langle S\rangle$ case [22]. The mass of the lightest Higgs boson h_1^0 remains below the bound (6.6) and approaches

$$m_{h_1^0}^2 \leq M_Z^2 \cos^2 2\beta + h_s^2 v^2 \left[\frac{1}{2}\sin^2 2\beta - \frac{h_s^2}{g'^2 Q_S^2} - 2\frac{\overline{Q}_H}{Q_S}\right]. \tag{6.7}$$

The limiting value (6.7) for $m_{h_1^0}$ can be larger or smaller than the MSSM upper bound $M_Z^2\cos^2 2\beta$, depending on couplings and charge assignments.

The pseudoscalar A^0 mass $m_{A^0}^2 \simeq \sqrt{2}Ah_s s/\sin 2\beta$ is expected to be large (unless Ah_s is very small), and one of the neutral scalars and the charged Higgs are then approximately degenerate with A^0, completing a full $SU(2)_L$ doublet $(H^0, A^0, H^\pm)$ not involved in $SU(2)_L$ breaking. The lightest neutral scalar is basically the (real part of the) neutral component of the Higgs doublet involved in $SU(2)_L$ breaking and has then a very small singlet component. The third neutral scalar has mass controlled by $M_{Z'}$ and is basically the singlet.

Most of these $U(1)'$ models require the existence of new heavy fermions carrying standard model charges to cancel anomalies [11], such as a heavy, $SU(2)$-singlet, quark $D_L + D_R$ with electric charge $-1/3$. These can be consistent with gauge unification if they fall into complete $SU(5)$ representations, as in the E_6 model [27]. The physics of a particular E_6 model is discussed in detail in [28, 29] and in Section 6.3. The Higgs sectors in $U(1)'$ models with a single Higgs field are compared and contrasted with other models involving a dynamical μ parameter in [30] and in Section 4 in this report.

In the single S model, $\langle S\rangle$ is responsible both for μ_{eff} and the Z' mass. The experimental lower limits on $M_{Z'}$ are model dependent, but are typically of order 600-900 GeV unless theZ' has very weak couplings to ordinary quarks and leptons. In the former case, there is a tension between obtaining a large enough Z' mass while generating the much lower electroweak scale [22, 27], requiring at least a small amount of tuning. This difficulty is resolved in the secluded sector models involving several S fields. In particular, one S, whose expectation value is comparable to that of the doublet Higgs fields, generates μ_{eff}, while all of the fields, some of which can have much larger expectation values, contribute to $M_{Z'}$. An explicit model in which this occurs naturally was constructed in [31]. In addition to the S field related to μ_{eff} there are three addition complex scalar fields $S_i, i = 1, 2, 3$, with superpotential

$$W = h_s S H_u H_d + \lambda S_1 S_2 S_3. \tag{6.8}$$

In the limit $\lambda \to 0$ there would be an F and D flat direction involving the S_i fields only, which would therefore acquire very large expectation values for appropriate soft breaking terms. For λ small but nonzero (e.g., 0.05), one finds $\langle S_i\rangle \sim m_{S_i}/\lambda$, where m_{S_i} is a soft mass, and large $M_{Z'}$. The secluded sector model has a very rich Higgs sector, involving 6 scalars and 4 pseudoscalars. (There can also be tree-level CP violation in the Higgs sector, which would lead to scalar-pseudoscalar mixing and with implications for baryogenesis [10].) The upper limit on the lightest scalar is relaxed, as in (6.6). However, the experimental *lower* limit of 114.4 GeV from LEP is also relaxed, because there can be considerable mixing between Higgs singlets and doublets (reducing the production rates), or the lightest scalar can be mainly singlet. There is often a light pseudoscalar, and low $\tan\beta$ values (e.g., $\sim 1-3$) are favored (these values are disfavored in the MSSM because of the Higgs mass limit). The Higgs sector was analyzed in detail in [32, 33] and in section 6.2. It was found in a parameter scan that the lightest Higgs could be as heavy as 168 GeV consistent with perturbatively to the Planck scale. A wide range of possibilities were found, depending on the parameters. These included both small and large values for the masses of the lightest scalar and pseudoscalar, and typically a fairly light neutralino. Many possibilities for

Higgs decays were found, including MSSM-like decays into $b\bar{b}$, etc., Higgs decays into lighter Higgs (e.g., scalar into two pseudoscalars), invisible decays into the lightest neutralino, and cascade decays involving a heavier neutralino. A particular limit of the model, in which three of the singlets essentially decouple, is discussed in [30]. There are three Higgs scalars, consisting mainly of S, H_d, and H_u, one of which can be light, and three additional singlets, one of which is very heavy (around $M_{Z'}$).

Many authors have considered the gauge group $SU(2)_L \times SU(2)_R \times U(1)_{B-L}$ [1], which may emerge as a subgroup of the grand-unified $SO(10)$ group. A principal motivation is that it allows a left-right interchange symmetry $\psi_L \leftrightarrow \psi_R$ between left and right-handed fermions, so that parity is broken spontaneously, with $SU(2)_R \times U(1)_{B-L}$ breaking to $U(1)_Y$ (weak hypercharge). Original versions assumed that both $SU(2)_R$ and the LR symmetry are broken at low energies (e.g., the TeV scale). However, there are variants (e.g., motivated by gauge unification) involving low scale $SU(2)_R$ breaking and high scale (e.g. 10^{10} GeV) LR breaking [34, 35]. It is also possible for both to be broken at a high scale, as may be necessary in some supersymmetric versions to avoid the spontaneous breaking of electric charge [36].

The simplest non-supersymmetric version involves a Higgs bi-doublet

$$\phi = \begin{pmatrix} \phi_1^0 & \phi_1^+ \\ \phi_2^- & \phi_2^0 \end{pmatrix}, \tag{6.9}$$

which transforms as $(2,2)$ under $SU(2)_L \times SU(2)_R$ with $B - L = 0$, and $\phi \leftrightarrow \phi^\dagger$ under the LR symmetry. The most popular version (which can also lead to a neutrino seesaw [1]) also introduces Higgs multiplets Δ_L, and Δ_R, which are respectively triplets under $SU(2)_L$ and $SU(2)_R$, with $B - L = 2$ and $\Delta_L \leftrightarrow \Delta_R$ under LR. They can be represented by the matrices

$$\Delta_{L,R} = \begin{pmatrix} \delta_{L,R}^+/\sqrt{2} & \delta_{L,R}^{++} \\ \delta_{L,R}^0 & -\delta_{L,R}^+/\sqrt{2} \end{pmatrix}. \tag{6.10}$$

The expectation values of the neutral components are

$$\begin{aligned} \langle\phi\rangle &= \begin{pmatrix} v_1/\sqrt{2} & 0 \\ 0 & v_2/\sqrt{2} \end{pmatrix} \\ \langle\Delta_{L,R}\rangle &= \begin{pmatrix} 0 & 0 \\ V_{L,R}/\sqrt{2} & 0 \end{pmatrix}, \end{aligned} \tag{6.11}$$

which may be complex. The $SU(2)_R$ breaking is due to $V_R^0 \gg v_{1,2}^0 \gg V_L^0$, while the normal electroweak breaking is from $v_{1,2}^0$. Variant forms of the model replace $\Delta_{L,R}$ by $\kappa_{L,R}$, which transform respectively as $(2,1)$ and $(1,2)$ under $SU(2)_L \times SU(2)_R$.

The Yukawa couplings are

$$-\mathcal{L}_{\text{Yukawa}} = \bar{\Psi}_L \left(\gamma\phi + \tilde{\gamma}\tilde{\phi}\right) \Psi_R + L_L^T C i\tau_2 \Gamma_L \Delta_L L_L + L_R^T C i\tau_2 \Gamma_R \Delta_R L_R + \text{h.c.} \tag{6.12}$$

where $\psi_{L,R}$ can be left (right) handed quark or lepton doublets, $L_{L,R}$ are lepton doublets, $\tilde{\phi} = \tau_2 \phi^* \tau_2$ is the charge-conjugated bi-doublet, and C is the charge conjugation matrix. γ and $\tilde{\gamma}$ are 3×3 Yukawa matrices (Hermitian by LR symmetry), while $\Gamma_{L,R}$ (equal by LR) are the 3×3 lepton-triplet couplings.

The minimal (non-supersymmetric) model in (6.12) therefore involves two Higgs doublets $\phi_{1,2}$ and two triplets $\Delta_{L,R}$. (More information on Higgs triplets may be found in Section 13.) After removing the Goldstone bosons eaten by the Higgs mechanism there are 14 physical Higgs degrees of freedom: 4 scalars, 2 pseudoscalars (which can mix with the scalars if CP is broken), two charged bosons and their charge conjugates, and two doubly charged bosons and their charge conjugates. Because the γ and $\tilde{\gamma}$ couplings will in general not be diagonalized by the same unitary transformations, the fermion

matrices will not be proportional to the physical Higgs-scalar Yukawa matrices (as in the standard model or MSSM). Therefore, the associated physical Higgs scalars will in general mediate flavor changing neutral currents. Explicit or spontaneous CP violation in the Higgs sector is also possible. Detailed studies of the Higgs sector include [37–44].

Supersymmetric generalizations of (6.12) cannot have the $\tilde{\gamma}$ term. (6.12) alone would then imply that the mass matrices for the charge $2/3$ and charge $-1/3$ quarks are proportional, leading to incorrect mass ratios and no CKM mixing. Such models would require either a second Higgs bi-doublet or other effects, such as significant soft supersymmetry breaking A terms associated with the Yukawa matrix, which however are not aligned with γ. There are also doubly charged Higgs triplets associated with $\Delta_{L,R}$. These could be light [36], even if $SU(2)_R$ is broken at a high scale, as is assumed in most supersymmetric studies. Implications of these doubly charged states for leptonic flavor changing processes and for collider physics have been studied, e.g., in [45] and [46] and in section 6.4. The Higgs structure of $SU(2)_L \times SU(2)_R \times U(1)_{B-L}$ is very rich. More systematic studies, especially of possible collider signatures, would be very useful.

6.1.2 Experimental signatures of Higgs bosons

Higgs boson phenomenology at future collider experiments can be illustrated using as an example the secluded $SU(2)_L \times U(1)_Y \times U(1)'$ model. The Higgs sector of this model consists of two MSSM like $SU(2)$ Higgs doublets and four additional Higgs singlets which are charged under an extra $U(1)'$ gauge symmetry. The spectrum of physical states comprises 6 CP-even scalars and 4 CP-odd states, denoted as H_1... H_6 and A_1...A_4, respectively, in order of increasing mass. One of the most striking features of this model is that A_1 is allowed to be very light, a feature shared with the NMSSM. To compare signatures of this model with the MSSM, it is convenient to introduce an "MSSM fraction" for a given state H_i (A_i)

$$\epsilon^i_{MSSM} = \sum_{j=1}^{2} (R^{ji})^2, \tag{6.13}$$

where R is the matrix relating interaction eigenstates to the mass eigenstates and j runs over MSSM states. When ϵ^i_{MSSM} = 1, the mass eigenstate contains no admixture of singlet Higgs bosons and approaches the properties of the MSSM Higgs boson. With increasing singlet fraction in the mass state, which corresponds to decreasing ϵ^i_{MSSM}, the Higgs state deviates in its properties from the MSSM Higgs boson. A large admixture of the singlet Higgs results in a reduced ZZH coupling,

$$g^2_{ZZH_i} = (R^{i1}_H \sin\beta - R^{i2}_H \cos\beta)^2 g^2_{ZZH,SM}, \tag{6.14}$$

relative to the standard model, where R_H is the matrix rotating CP-even interaction eigenstates to the mass basis. As a consequence, the Higgs-strahlung cross section is reduced with respect to the SM expectation, allowing a relaxation of the lower limit of 114 GeV from LEP.

Due to rather distinctive features of the Higgs sector from the SM and MSSM, it is important to study decay properties of the lightest CP-even and CP-odd Higgs bosons in order to explore their possible observation at future collider experiments. For the lightest CP-even Higgs boson with a mass below approximately 100 GeV, the LEP constraints require the Higgs to be mostly singlet. Thus, the decay modes to A_1A_1 and $\tilde{\chi}^0_1\tilde{\chi}^0_1$ are dominant when they are kinematically allowed, due to the presence of the extra $U(1)'$ gauge coupling and trilinear superpotential terms proportional to h_s and λ (Eq. 6.8). If these channels are kinematically disallowed, the properties of the lightest CP-even state become similar to those of MSSM Higgs bosons and decays to the heaviest SM fermions, $b\bar{b}$, $c\bar{c}$ and $\tau^+\tau^-$ become dominant. When the lightest scalar is heavier than the LEP2 bound, it may have a substantial "MSSM fraction" and can decay to A_1A_1 and $\tilde{\chi}^0_1\tilde{\chi}^0_1$ and SM particles. The light A_1 will decay dominantly to neutralinos when it is kinematically possible. Otherwise the A_1 decays into the heaviest accessible fermions, which are usually b quarks, unless A_1 is lighter than the $b\bar{b}$ pair mass. Charm and tau decays can

also be significant, depending on $\tan\beta$. For heavy $A_1 \geq 200$ GeV, decays to neutralinos and charginos universally dominate due to their gauge strength, suppressing $b\bar{b}$ below 10%. The A_1 and H_1 bosons can be lighter than $\tilde{\chi}_1^0$. However, in models with R-parity conservation, decays of $\tilde{\chi}_1^0$ to Higgs bosons are not allowed and the lightest neutralino is considered to be the lightest stable supersymmetric particle. Hence, the decay of lightest Higgs states into neutralinos are assumed to be invisible.

If Higgs bosons are discovered at the LHC, the linear collider will be an ideal machine to probe this class of models and disentangle them from the SM or MSSM. If due to specific decay modes the observation of Higgs bosons will be difficult at the LHC, the linear collider will serve as a discovery machine.

In electron-positron collisions the dominant production mechanisms for CP-even Higgs bosons are Higgs-strahlung, $e^+e^- \rightarrow ZH_i$, and W-fusion, $e^+e^- \rightarrow \nu\bar{\nu}H_i$ processes. The cross sections of these processes are reduced compared to the SM cross sections by a factor $(R_H^{i1}\sin\beta - R_H^{i2}\cos\beta)^2$, as in (6.14). As can be seen, the SM Higgs-strahlung cross section gets suppressed for a small amount of mixing into SM-like or MSSM-like Higgs for a given Higgs state and vanishes when the Higgs boson is mostly singlet. The CP-odd states are produced mainly through the Higgs pair production mechanism, $e^+e^- \rightarrow H_iA_j$, with the cross section given by

$$\sigma(e^+e^- \rightarrow H_iA_j) = (R_H^{i1}R_A^{j1} - R_H^{i2}R_A^{j2})^2 K\sigma_{SM}(e^+e^- \rightarrow Zh), \tag{6.15}$$

where R_A is the matrix that diagonalizes the CP-odd Higgs mass matrix, $\sigma_{SM}(e^+e^- \rightarrow Zh)$ is the SM cross section for Higgs-strahlung, and K is a kinematic factor given in [32].

The Higgs phenomenology at future colliders depends on the specific model point, defining Higgs boson mass spectrum, their production cross section and decay branching ratios. In the following we consider a set of representative scenarios, reflecting various experimental signatures in this class of models.

MSSM like scenario

When MSSM fractions are close to one, the model is MSSM like, with the production rates and decay modes similar to those expected in the MSSM. The observation of Higgs states is possible in the standard discovery channels anticipated for the SM and MSSM, even if production rates are reduced due to the admixture of the singlet component for a given Higgs state.

Multijet final states

For some parameter choices, the decay modes $H_i \rightarrow H_jH_j$ or $H_i \rightarrow A_jA_j$ become dominant, with subsequent decays of H_j and A_j into hadrons or tau-leptons. This scenario provides a challenge for the LHC because of large QCD backgrounds. At the linear e^+e^- collider, the rich spectrum of signal topologies will be available for the detection of Higgs bosons.

The most promising channel is the Higgs-strahlung followed by decays of Z into e^+e^- and $\mu^+\mu^-$. The signal can be identified as the peak in the mass distribution of the system recoiling against the dilepton pair. The multi-jet channels, such as

- $H_1A_1 \rightarrow 4\,jets$,
- $ZH_2 \rightarrow q\bar{q}H_1H_1, q\bar{q}A_1A_1 \rightarrow 6\,jets$,
- $H_2A_1, H_1A_2 \rightarrow 6\,jets$,
- $H_2A_2 \rightarrow 8\,jets$

can also be exploited to detect Higgs bosons and measure their properties. Excellent performance of the vertex detector is very crucial for identification of these final states as they will include b or c quarks, stemming from the light CP-even and CP-odd Higgs decays. Good capability of identifying vertex charges would also be desirable as it will allow a reduction of the combinatorial background in multi-jet final states.

Invisible decays

Scenarios are possible when MSSM or SM decay modes of H_i states are suppressed to the benefit of the $H_i \to \tilde{\chi}^0_1\tilde{\chi}^0_1, A_jA_j, H_jH_j$ channels with A_j and H_j decaying into the lightest neutralino. This scenario will present a challenge at the LHC. At the LC, however, the reconstruction of the mass peak is possible exploiting the Higgs-strahlung process followed by a visible decay of the Z, $Z \to q\bar{q}, e^+e^-, \mu^+\mu^-$. Dedicated analyses showed [47] that the invisible branching ratio of the Higgs can be measured with a relative precision of few % down to $Br(H \to inv.)$ = 0.1 for Higgs masses up to 160 GeV. This result is obtained for a Higgs-strahlung cross section close to the value expected in the SM.[1]

Cascade decays involving supersymmetric particles

For certain model parameter points one or more Higgs bosons can decay into heavy neutralinos. In this case, cascade decays of $\tilde{\chi}^0_{i>1}$ to the LSP will produce multi-fermion final states which may include both jets and leptons accompanied by large missing energy.

The class of models with extra gauge groups significantly enriches the Higgs boson phenomenology compared to the SM or MSSM. At this point it should emphasized that efficient identification of exotic channels, involving multi-jet final states, invisible decays and cascade decays of Higgs bosons to the LSP will be of crucial importance for disentangling these models from the SM and MSSM.

Constraints from Z' Searches

Results from searches for extra gauge bosons constrain $U(1)'$ models. Dilepton searches at the Tevatron require $M_{Z'} > 600 - 900$ GeV, depending on the model [48], while results from weak neutral currents and LEP2 [49] restrict the Z' mass and mixing. The strongest restrictions arise from the mixing between Z and Z' induced by electroweak symmetry breaking:

$$\alpha_{Z-Z'} = \frac{1}{2}\arctan\left(\frac{2M^2_{ZZ'}}{M^2_{Z'} - M^2_Z}\right), \tag{6.16}$$

with the off-diagonal entry $M^2_{ZZ'}$ and the diagonal elements $M^2_{Z'},\ M^2_Z$ in the mass-squared matrix. For typical models the $Z - Z'$ mixing is restricted by measurements at the Z resonance to be less than a few 10^{-3} [49–51]. The small $Z - Z'$ mixing angle requires $M_{Z'} \gg M_Z$ or, with respect to existing results, $M_{Z'} > 500$ GeV.

If the fermions receive mass through the usual Higgs mechanism some of them must be charged under $U(1)'$ to keep the superpotential Yukawa terms gauge invariant (assuming the Higgs fields are charged). The exact Z' production cross section depends on the fermion $U(1)'$ charges, but bosons with $M_{Z'} > 500$ GeV would be produced at tree level at the Tevatron and future colliders.

Z' models as constructed in [31, 32] can easily be satisfied for $M_{Z'}$ in the TeV range. Even higher $M_{Z'}$ values are allowed for large vacuum expectation values. Accordingly, the Z' bosons can also be light if the singlets have smaller vacuum expectation values. This is possible since the singlets do not couple directly to the Standard Model.

In general, establishing the existence of new $U(1)'$ gauge symmetries necessitates experimental evidence also for Z' bosons. Distinguishing different $U(1)'$ models would require certain signatures based on the nature of Z' couplings which are not considered in this context of Higgs studies here.

[1] Invisible Higgs decays occur in a variety of models and are discussed in detail in the context of large extra dimensions in Section 8.

6.2 The Higgs sector in a secluded sector $U(1)'$ model

Tao Han, Paul Langacker and Bob McElrath

6.2.1 The model

6.2.1.1 General structure

The model we [32] consider, first introduced in [31], has the superpotential:

$$W = hSH_uH_d + \lambda S_1S_2S_3 + W_{\rm MSSM}|_{\mu=0} \tag{6.17}$$

S, S_1, S_2, and S_3 are standard model singlets, but are charged under an extra $U(1)'$ gauge symmetry. The off-diagonal nature of the second term is inspired by string constructions, and the model is such that the potential has an F and D-flat direction in the limit $\lambda \to 0$, allowing a large (TeV scale) Z' mass for small λ. The use of an S field different from the S_i in the first term allows a decoupling of $M_{Z'}$ from the effective μ. W leads to the F-term scalar potential:

$$\begin{aligned} V_F = &\quad h^2\left(|H_u|^2|H_d|^2 + |S|^2|H_u|^2 + |S|^2|H_d|^2\right) \\ + &\quad \lambda^2\left(|S_1|^2|S_2|^2 + |S_2|^2|S_3|^2 + |S_3|^2|S_1|^2\right) \end{aligned} \tag{6.18}$$

The D-term potential is:

$$\begin{aligned} V_D &= \frac{G^2}{8}\left(|H_u|^2 - |H_d|^2\right)^2 \\ &+ \frac{1}{2}g_{Z'}^2\left(Q_S|S|^2 + Q_{H_d}|H_1|^2 + Q_{H_u}|H_u|^2 + \sum_{i=1}^{3} Q_{S_i}|S_i|^2\right)^2 , \end{aligned} \tag{6.19}$$

where $G^2 = g_1^2 + g_2^2 = g_2^2/\cos^2\theta_W$. g_1, g_2, and $g_{Z'}$ are the coupling constants for $U(1), SU(2)$ and $U(1)'$, respectively, and θ_W is the weak angle. Q_ϕ is the $U(1)'$ charge of the field ϕ. We will take $g_{Z'} \sim \sqrt{5/3}g_1$ (motivated by gauge unification) for definiteness.

We do not specify a SUSY breaking mechanism but rather parameterize the breaking with the soft terms

$$\begin{aligned} V_{\rm soft} &= m_{H_d}^2|H_d|^2 + m_{H_u}^2|H_u|^2 + m_S^2|S|^2 + \sum_{i=1}^{3} m_{S_i}^2|S_i|^2 \\ &- (A_h hSH_uH_d + A_\lambda\lambda S_1S_2S_3 + \text{H.C.}) \\ &+ (m_{SS_1}^2 SS_1 + m_{SS_2}^2 SS_2 + \text{H.C.}) \end{aligned} \tag{6.20}$$

The last two terms are necessary to break two unwanted global $U(1)$ symmetries, and require $Q_{S_1} = Q_{S_2} = -Q_S$. The potential $V = V_F + V_D + V_{soft}$ was studied in [31], where it was shown that for appropriate parameter ranges it is free of unwanted runaway directions and has an appropriate minimum. We denote the vacuum expectation values of H_i, S, and S_i by v_i, v_s, and v_{si}, respectively, i.e., without a factor of $1/\sqrt{2}$. Without loss of generality we can choose $A_h h > 0$, $A_\lambda\lambda > 0$ and $m_{SS_i}^2 < 0$ in which case the minimum occurs for the expectation values all real and positive.

So far we have only specified the Higgs sector, which is the focus of this study. Fermions must also be charged under the $U(1)'$ symmetry in order for the fermion superpotential Yukawa terms $W_{fermion} = \bar{u}\mathbf{y_u}QH_u - \bar{d}\mathbf{y_d}QH_d - \bar{e}\mathbf{y_e}LH_d$ to be gauge invariant. The $U(1)'$ charges for fermions do not contribute significantly to Higgs production or decay, if sfermions and the Z' superpartner are heavy. We therefore ignore them in this study.

Anomaly cancellation in $U(1)'$ models generally requires the introduction of additional chiral supermultiplets with exotic SM quantum numbers [2, 10, 11, 22, 27, 52]. These can be consistent with

gauge unification, but do introduce additional model-dependence. The exotics can be given masses by the same scalars that give rise to the heavy Z' mass. The exotic sector is not the focus of this study. We therefore consider the scenario in which the Z' and other matter necessary to cancel anomalies is too heavy to significantly affect the production and decays of the lighter Higgs particles.

6.2.1.2 Higgs sector and electroweak symmetry breaking

The Higgs sector for this model contains 6 CP-even scalars and 4 physical CP-odd scalars, which we label $H_1 ... H_6$ and $A_1 ... A_4$, respectively, in order of increasing mass.

We find viable electroweak symmetry breaking minima by scanning over the vacuum expectation values of the six CP-even scalar fields. We require that the CP-even mass matrix be positive definite numerically, which guarantees a local minima, while simultaneously eliminating the soft mass squared for each field. The masses reported are evaluated including the dominant 1-loop correction coming from the top and stop loops. The CP-odd mass matrix is guaranteed to be positive semi-definite at tree level (and thus, all VEV's are real) by appropriate redefinitions of the fields and choices of parameters.

We scan over vacuum expectation values such that the three singlets S_1, S_2, and S_3 typically have larger VEV's than the other three fields. We allow points in our Monte Carlo scan that fluctuate from all VEV's equal up to $\langle S \rangle$ approximately 1 TeV and $\langle S_i \rangle$ approximately 10 TeV. This generically results in a spectrum with 1-5 relatively light CP-even states, often with one of them lighter than the LEP2 mass bound, but having a relatively small mixing with the MSSM H_u and H_d. It is necessary that at least one of the singlets have an $\mathcal{O}(\mathrm{TeV})$ vacuum expectation value, so that the mass of the Z' gauge boson is sufficently heavy that it evades current experimental bounds, and any extra matter needed to cancel anomalies is heavy enough to not significantly affect light Higgs production or decay.

A bound exists on the mass of the lightest Higgs particle in any perturbatively valid supersymmetric theory [18, 53]. The limit on the lightest MSSM-like CP-even Higgs mass in this model is:

$$\begin{aligned} M_h^2 \leq h^2 v^2 &+ (M_Z^2 - h^2 v^2) \cos^2 2\beta + 2 g_{Z'}^2 v^2 (Q_{H_u} \cos^2 \beta + \sin^2 \beta Q_{H_d})^2 \\ &+ \frac{3}{4} \frac{m_t^4}{\pi^2 v^2} \ln \frac{m_{\tilde{t_1}} m_{\tilde{t_2}}}{m_t^2}. \end{aligned} \tag{6.21}$$

This is obtained by taking the limit as the equivalent of the B-term in the MSSM goes to infinity, $B = A_h h v_s \to \infty$, in the 2×2 submatrix containing H_u and H_d. In the MSSM this is equivalent to taking $M_A \to \infty$, the decoupling limit. This expression is the same as in the NMSSM, except for the $g_{Z'}$ (D-term) contribution. Perturbativity to a GUT or Planck scale places an upper limit $\mathcal{O}(0.8)$ on h [31], which is less stringent than the corresponding limit in the NMSSM [54–56] due to the $U(1)'$ contributions to its renormalization group equations. Larger values would be allowed if another scale entered before the Planck scale. We will allow h as large as 1 in the interest of exploring the low energy effective potential. The second term of Eq. (6.21) vanishes for $\tan\beta = 1$. Since $\tan\beta \simeq 1$ generically in these models, the lightest Higgs mass is determined mostly by the new F and D-term contributions proportional to h^2 and $g_{Z'}^2$. In this model, as with any model with many Higgs particles, a situation can arise in which the MSSM-like couplings are shared among many states, allowing unusually heavy states or unusually light states that evade current experimental bounds.

The four CP-odd masses can in principle be found algebraically but the results are complicated and not very illuminating. Perhaps the most striking feature of the mass spectrum is that the A_1 is allowed to be very light, a feature shared with the NMSSM [57–63]. This can lead to a much lighter CP-even higgs due to $H_1 \to A_1 A_1$ decays [64, 65] and very light dark matter due to the new s-channel annihilation through the A_1 [66]. This light A_1 is caused by a combination of small $m_{SS_1}^2$ or $m_{SS_2}^2$ and a small value of v_s compared to the v_{si}. In the limit that v_{si} ($i = 1$ or 2) is the largest scale in the problem, the lightest A mass is

$$m_{A_1}^2 = -m_{SS_i}^2 \frac{v_s v_{si}}{v_{si}^2 + v_{s3}^2} + \mathcal{O}\left(\frac{1}{v_{si}^4}\right). \tag{6.22}$$

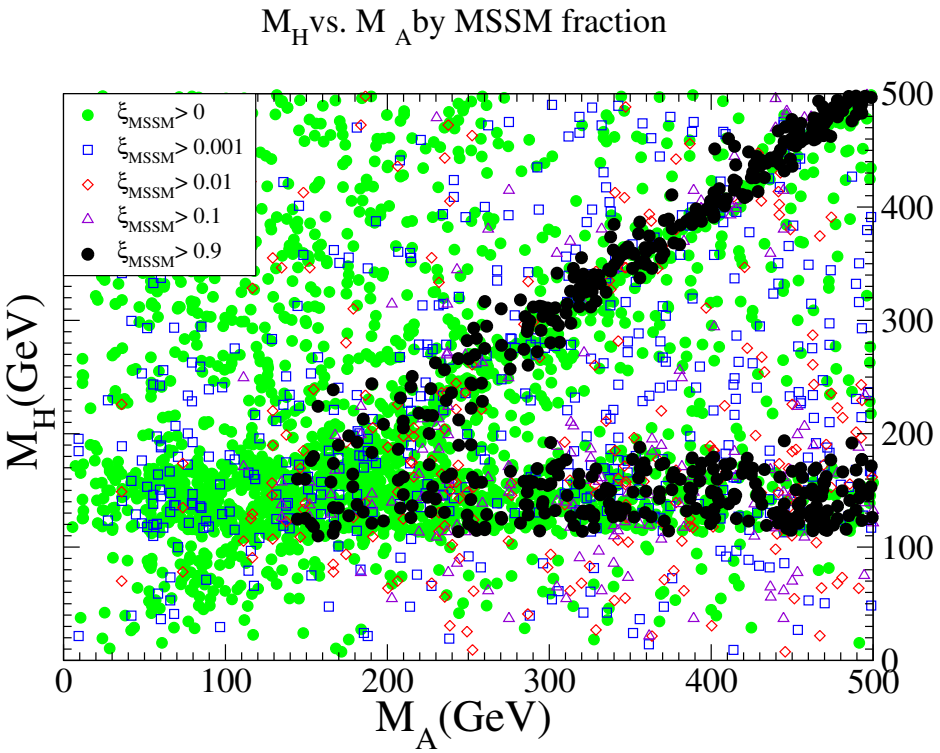

Fig. 6.1: $M_H - M_A$ mass plane, labeled according to MSSM fraction $\xi_{\rm MSSM}$. For each point both H_i and A_i satisfy the condition $\xi_{\rm MSSM} > 0, 0.001, 0.01, 0.1$, or 0.9. All pairs (M_{H_i}, M_{A_j}) are plotted.

In the limit that s_3 is large we obtain

$$m^2_{A_1} = -4m^2_{SS_i}\frac{v_s v_{si}}{v_s^2 + v_{s1}^2 + v_{s2}^2} + \mathcal{O}\left(\frac{1}{v_{s3}}\right). \tag{6.23}$$

In our scans, $-m^2_{SS_i}$ is approximately in the range $(0 - 1000\ \text{GeV})^2$. However, this requires a hierarchy between the off-diagonal soft masses m_{SS_i} and the other soft masses m_S and m_{S_i}. This might be difficult to achieve depending on the SUSY breaking mechanism. A similar analysis holds for H_1, but an algebraic expression cannot be derived since the eigenvalues of a 6×6 matrix cannot be expressed algebraically.

6.2.2 Phenomenological constraints

Due to the introduction of the Higgs singlets, there are several more parameters than in the MSSM Higgs sector. We follow the global symmetry breaking structure of Model I of Ref. [31]. Existing experimental measurements already constrain any new model. In our parameter space scans, we apply the constraints as outlined in Ref. [32]. All the model points shown on our figures are consistent with all the important constraints from LEP2.

6.2.3 Mass spectrum and couplings for Higgs bosons

We first point out the relaxed upper bound on the mass of the lightest CP-even Higgs boson. As given in Eq. (6.21), the lightest CP-even Higgs boson mass at tree level would vanish in the limit $h \to 0$, $g_{Z'} \to 0$ and $\tan\beta \to 1$. Using the parameters discussed in Ref. [32], the upper limit on the lightest Higgs boson mass at tree level as given by the first two terms in Eq. (6.21) is $142\,\text{GeV}$. Including the effects of Higgs mixing and the one-loop top correction, we find masses up to $\sim 168\,\text{GeV}$. The mass could be made even larger if we allowed $h > 1$, although the perturbativity requirement up to the GUT

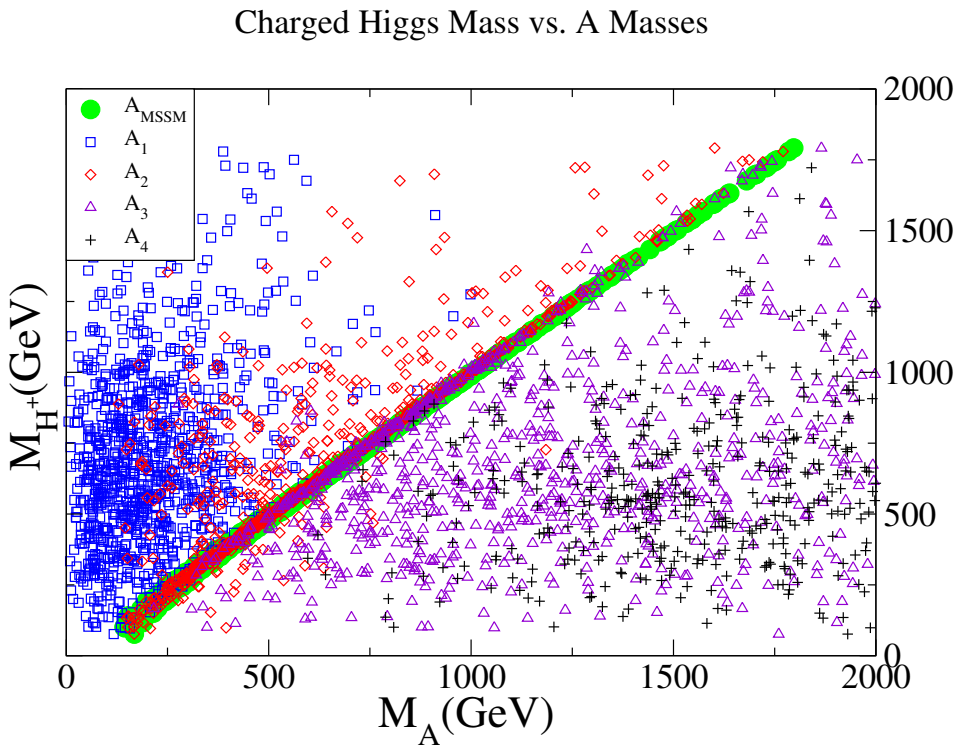

Fig. 6.2: $M_{H^+} - M_A$ mass plane with the MSSM $A^{\rm MSSM}$ mass $M_A^{\rm MSSM} = 2A_h h v_s / \sin 2\beta$ included for comparison. All pairs (M_{H_i}, M_{A_j}) are plotted.

scale at 1-loop level would imply that $h \leq 0.8$. We know that new heavy exotic matter must enter this model to cancel anomalies, so it is not necessarily justified to require h to be perturbative to the Planck scale by calculating its 1-loop running using only low energy fields.

The masses of the various Higgs particles are a function of the mixing parameters, and most of the simple MSSM relations among masses are broken. It is quite common to have a light singlet with sizable MSSM fraction that can still evade the LEP2 bounds. Typical allowed light CP-even and odd masses are shown in Fig. 6.1 for various ranges of MSSM fractions. We see that it is possible to have light MSSM Higgs bosons below about 100 GeV without conflicting the LEP2 searches. This is because of the reduced couplings to the Z when the MSSM fraction becomes small. One can clearly make out the usual MSSM structure when $\xi_{\rm MSSM}$ is large, with the diagonal band for $\xi_{\rm MSSM} > 0.9$ being $M_H^{\rm MSSM} \simeq M_A^{\rm MSSM}$, and the horizontal band being the saturation of $M_h^{\rm MSSM}$ at its upper bound in the decoupling limit. As ξ_{MSSM} decreases, we can see points in the lower left that are able to evade the LEP2 bounds on $M_{h,H}$ and M_A.

The mass range for the charged Higgs boson is demonstrated in Fig. 6.2. There is still a linear relationship between the charged Higgs mass and the MSSM A mass since the singlets do not affect the H^+ mass. However, after mixing there is not necessarily a state with that mass, or the identity of the state is obscured. Most of the parameter space has a single state that can be identified as MSSM-like, with $\xi_{\rm MSSM} \sim 1$; in such circumstances there is also generally an H very close in mass to both the A and H^+. However, the difference between M_{H^+} and the M_{A_i} can be 50 GeV or more due to mixing, especially when the MSSM-like state is not clearly identifiable.

One of the most important parameters in the SUSY Higgs sector is $\tan\beta$. In the model under consideration, $\tan\beta \approx 1$ is favored (because A_h must be large enough to ensure $SU(2)$ breaking).

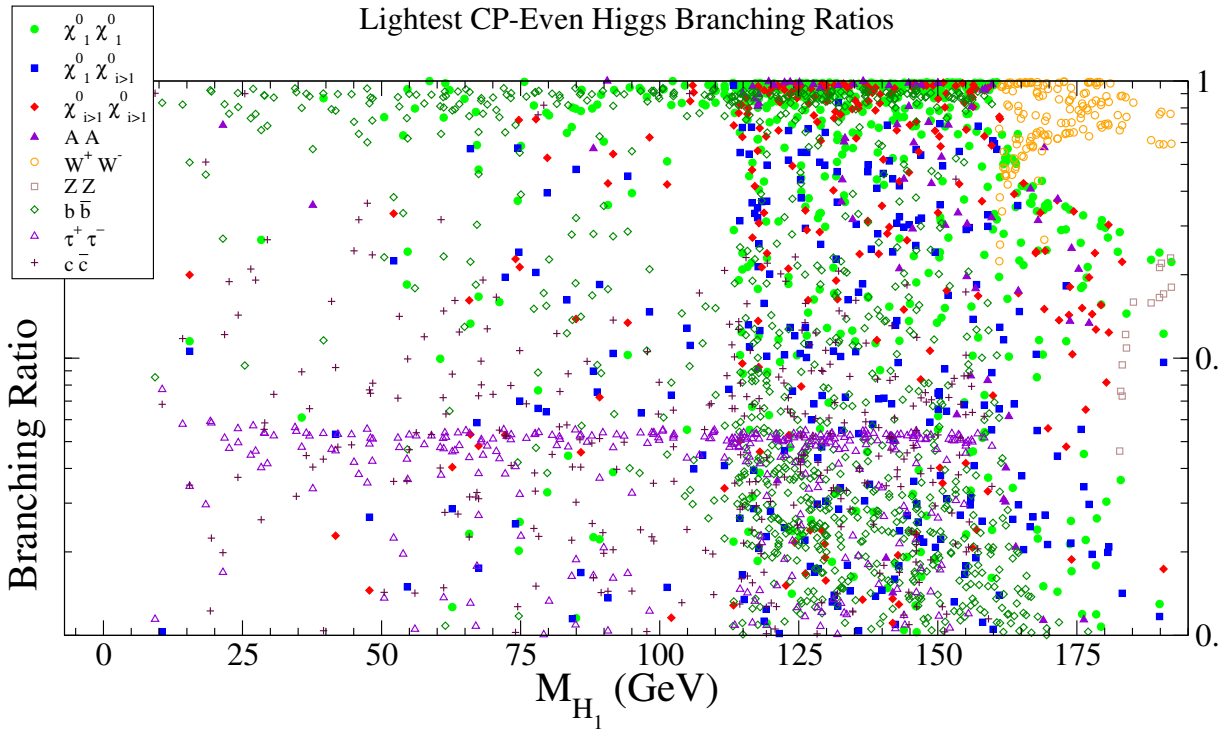

Fig. 6.3: Branching ratios of the lightest CP-even Higgs.

6.2.4 Higgs boson decay and production in e^+e^- collisions

Due to the rather distinctive features of the Higgs sector different from the SM and MSSM, it is important to study how the lightest Higgs bosons decay in order to explore their possible observation at future collider experiments. The lightest Higgs bosons can decay to quite non-standard channels, leading to distinctive, yet sometimes difficult experimental signatures. For the Higgs boson production and signal observation, we concentrate on an e^+e^- linear collider. It is known that a linear collider can provide a clean experimental environment to sensitively search for and accurately study new physics signatures. If the Higgs bosons are discovered at the LHC, a linear collider would be needed to disentangle the complicated signals in this class of models. If, on the other hand, a Higgs boson is not observed at the LHC due to the decay modes difficult to observe at the hadron collider environment, a linear collider will serve as a discovery machine.

6.2.4.1 Lightest CP-even state H_1

The main decay modes and corresponding branching fractions for the lightest CP-even Higgs H_1 are presented in Fig. 6.3(left). For lightest Higgs masses below approximately 100 GeV, the LEP2 constraint is very tight, and the lightest Higgs must be mostly singlet. Thus, the decay modes to A_1A_1 and $\chi^0_1\chi^0_1$ are dominant when they are kinematically allowed, due to the presence of the extra $U(1)'$ gauge coupling and trilinear superpotential terms proportional to h and λ. When those modes are not kinematically accessible, the decays are very similar to the MSSM modulo an eigenvector factor that is essentially how much of H_u and H_d are in the lightest state. Therefore $b\bar{b}$, $c\bar{c}$ and $\tau^+\tau^-$ decays dominate, with $c\bar{c}$ and $\tau^+\tau^-$ approximately an order of magnitude smaller than $b\bar{b}$, due to the difference in their Yukawa couplings. Since $\tan\beta \approx 1$, the $c\bar{c}$ mode can be competitive with both $\tau^+\tau^-$ and $b\bar{b}$ since their masses are similar. In the MSSM the $c\bar{c}$ mode is suppressed because $\tan\beta$ is expected to be larger.

When the lightest Higgs is heavier than the LEP2 bound, it does not need to be mostly singlet, and there can be a continuum of branching ratios to A_1A_1, $\chi^0_1\chi^0_1$ or SM particles, depending on how much

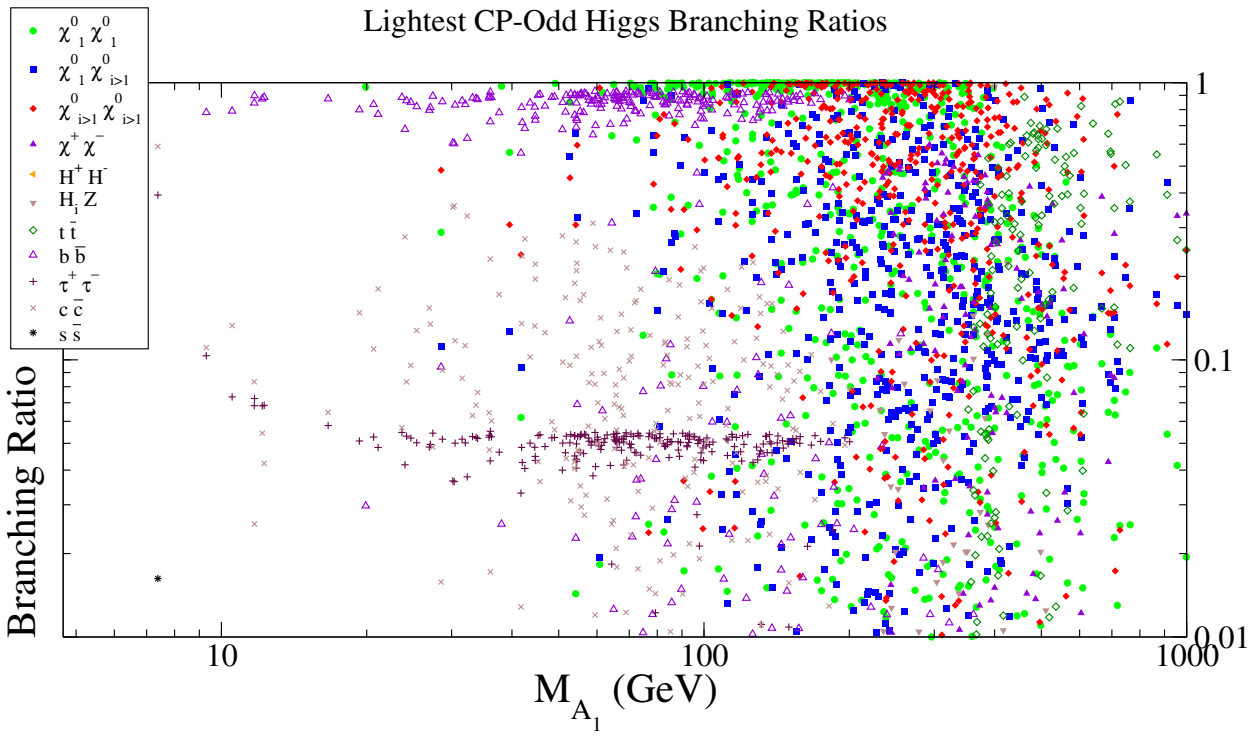

Fig. 6.4: Branching ratios for the lightest CP-odd Higgs.

singlet is in the lightest state. This is indeed seen in Fig. 6.3(right) for a heavier H_1 where the modes $H_1 \to W^+W^-,\ ZZ$ become substantial.

A striking feature of this graph is that the usual "discovery" modes for $M_{H_1} < 140$, $H_1 \to b\bar{b},\ \tau^+\tau^-$ are often strongly suppressed by decays to A_1 and χ^0_1. Only $H_1 \to W^+W^-,\ ZZ$ decays are able to compete with the new A_1 and χ^0_1 decays, which are all of gauge strength. One can see that the traditional shape of the W^+W^- and ZZ threshold is obscured by the presence of χ^0_1 and A decays, depending on what is kinematically accessible. For a H_1 heavy enough for these decay modes to be open, however, the coupling h is typically greater than 0.8, large enough that it will become non-perturbative before the Planck scale unless new thresholds enter at a lower scale to modify its running.

The A_1 or H_1 can be lighter than the χ^0_1. However, we assume R-parity is conserved. Therefore, decays of χ^0_1 to A_1 or H_1 are not allowed and the lightest neutralino is assumed to be the (stable) LSP. We do not analyze the sfermion sector, which can produce a sfermion LSP in some regions of parameter space, but these scenarios are phenomenologically disfavored. We therefore assume H and A decays to χ^0_1 are invisible at a collider. We separate the heavier neutralinos $\chi^0_{i>1}$ which may decay visibly [67].

6.2.4.2 CP-odd

The decays of the CP-odd Higgs bosons are presented in Fig. 6.4. The light A_1 will decay dominantly to neutralinos when it is kinematically possible. When it is not, it decays dominantly into the nearest mass SM fermion, which is usually b unless the A_1 is lighter than the $b\bar{b}$ pair mass. Charm and tau decays can also be significant, depending on the value of $\tan\beta$. The $c\bar{c}$ decays are about 3 times more likely than the $\tau^+\tau^-$ due to the color factor. However, for larger $\tan\beta$ the $\tau^+\tau^-$ dominates.

For heavy $A_1 \gtrsim 200$ GeV, decays to neutralinos and charginos universally dominate due to their gauge strength, suppressing the $b\bar{b}$ mode below 10%.

The lightest A can decay only into light SM fermions, the photon, and neutralinos. Hadronic bottom and charm decays are difficult to separate from background, and τ's are obscured by missing

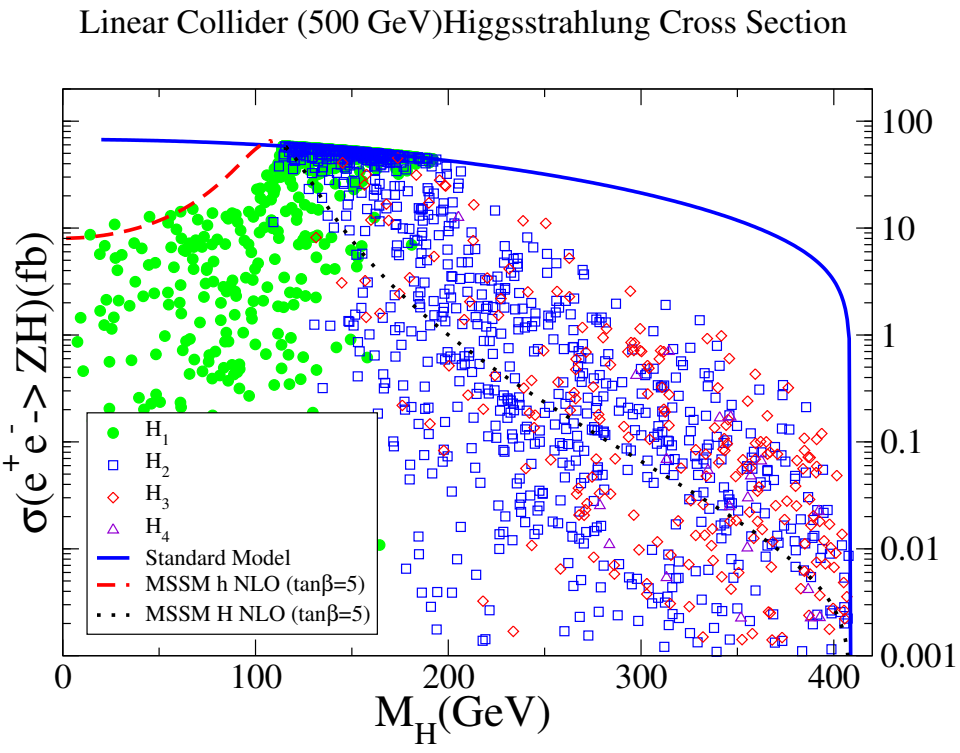

Fig. 6.5: Cross section at a 500 GeV linear collider for ZH_i production. The solid curve is the SM production, and the dashed and dot-dashed for MSSM h and H production with $\tan\beta = 5$.

energy and hadronic background.

6.2.4.3 The Higgs signatures at a linear collider

The production via radiation of a Higgs from a virtual Z boson is the dominant mechanism for CP-even Higgs production at a linear collider. We show this cross section in Fig. 6.5, where each point is a viable model solution satisfying all the constraints. The curves present the SM and MSSM cross sections for comparison. Model points with $M_H < 114.1$ are only those with suppressed coupling to the Z, and those with large MSSM fraction are removed by the LEP2 bounds. The ratio between the Standard Model cross section and that for any model point simply reflects the amount of mixing into the SM-like or MSSM-like Higgs for a given Higgs state.

The production cross sections for the heavier Higgs particles are very small. For heavy states (that correspond to the H in MSSM), $\cos(\alpha - \beta) \to 0$ as the H gets heavier. In this decoupling limit of the MSSM the heavy H has no coupling to the Z.

At 500 GeV the weak boson fusion production modes $e^+e^- \to \nu\bar{\nu}H$, e^+e^-H are comparable in size to the Higgsstrahlung mode. At higher energies, the weak boson fusion becomes larger than Higgsstrahlung and is the most important production mode. These curves are similar to Fig. 6.4(b), reflecting that all of these single Higgs production modes are simply a mixing factor times the Standard Model curve. It is particularly interesting to note that the ZZ fusion channel $e^+e^- \to e^+e^-H$ can serve as a model-independent process to measure the ZZH coupling regardless the decay of H, even if H is invisible [68].

As anticipated for the next generation linear collider with $\sqrt{s} = 500$ GeV and an integrated luminosity of the order of $500 - 1000$ fb^{-1}, one should be able to cover a substantial region of the parameter space. For instance, with a cross section of the order of 0.1 fb, this may lead to about $50-100$ events. As for further exploration of signal searches, it depends on specific model parameters. We have

provided a comprehensive list of representative models in the Appendices of Ref. [32].

It is clear that the model studied in this paper presents very rich physics in the Higgs sector. An e^+e^- linear collider will be ideally suited for the detailed exploration of the non-standard Higgs physics. Analyses for the LHC should also be performed, particularly for the non-MSSM modes [69, 70].

6.3 Higgs spectrum in the exceptional supersymmetric standard model

Steve F. King, Stefano Moretti and Roman Nevzorov

6.3.1 The model

A solution to the μ-problem discussed in the Introduction of this section naturally arises within superstring inspired models based on the E_6 gauge group. At the string scale, E_6 can be broken directly to the rank-6 subgroup $SU(3)_C \times SU(2)_L \times U(1)_Y \times U(1)_\psi \times U(1)_\chi$ via the Hosotani mechanism [71]. Two anomaly-free $U(1)_\psi$ and $U(1)_\chi$ symmetries of the rank-6 model are defined by: $E_6 \to SO(10) \times U(1)_\psi$, $SO(10) \to SU(5) \times U(1)_\chi$. Near the string scale the rank-6 model can be reduced further to an effective rank-5 model with only one extra $U(1)'$ gauge symmetry. Thus in general the extra $U(1)'$ that appears at low energies in superstring inspired models is a linear combination of $U(1)_\chi$ and $U(1)_\psi$, i.e. $U(1)' = U(1)_\chi \cos\theta + U(1)_\psi \sin\theta$. If $\theta \neq 0$ or π the extra $U(1)'$ gauge symmetry forbids an elementary μ-term but allows the interaction $h_s S H_d H_u$ in the superpotential. After electroweak symmetry breaking (EWSB) the scalar component of the standard model (SM) singlet superfield S acquires a non-zero vacuum expectation value (VEV) breaking $U(1)'$ and giving rise to an effective μ term.

Here we explore the Higgs sector of a particular E_6 inspired supersymmetric model with extra $U(1)_N$ gauge symmetry in which right handed neutrinos do not participate in the gauge interactions ($\theta = \arctan\sqrt{15}$). Only in this exceptional supersymmetric standard model (E_6SSM) right-handed neutrinos may be superheavy, shedding light on the origin of the mass hierarchy in the lepton sector and providing a mechanism for the generation of lepton and baryon asymmetry of the Universe [28]- [29]. Recently the implications of SUSY models with an additional $U(1)_N$ gauge symmetry have been studied for the neutrino physics [72]- [73], leptogenesis [74] and electroweak baryogenesis [75]. Previously supersymmetric models with an extra $U(1)_N$ factor have been also considered in [76]- [77] in the context of $Z - Z'$ mixing and a discussion of the neutralino sector and in [24] where the one-loop upper bound on the lightest Higgs was examined.

To ensure anomaly cancellation the particle content of the E_6SSM should include complete fundamental 27 representations of E_6. These multiplets decompose under the $SU(5) \times U(1)_N$ subgroup of E_6 [78] as follows:

$$27_i \to \left(10, \frac{1}{\sqrt{40}}\right)_i + \left(5^*, \frac{2}{\sqrt{40}}\right)_i + \left(5^*, -\frac{3}{\sqrt{40}}\right)_i + \left(5, -\frac{2}{\sqrt{40}}\right)_i + \left(1, \frac{5}{\sqrt{40}}\right)_i + (1,0)_i\,. \tag{6.24}$$

The first and second quantities in the brackets are the $SU(5)$ representation and extra $U(1)_N$ charge while i is a family index that runs from 1 to 3. An ordinary SM family which contains the doublets of left-handed quarks Q_i and leptons L_i, right-handed up- and down-quarks (u_i^c and d_i^c) as well as right-handed charged leptons, is assigned to $\left(10, \frac{1}{\sqrt{40}}\right)_i + \left(5^*, \frac{2}{\sqrt{40}}\right)_i$. Right-handed neutrinos N_i^c should be associated with the last term in Eq. (6.24), $(1,0)_i$. The next-to-last term in Eq. (6.24), $\left(1, \frac{5}{\sqrt{40}}\right)_i$, represents SM-type singlet fields S_i which carry non-zero $U(1)_N$ charges and therefore survive down to the EW scale. The pair of $SU(2)$-doublets (H_{1i} and H_{2i}) that are contained in $\left(5^*, -\frac{3}{\sqrt{40}}\right)_i$ and $\left(5, -\frac{2}{\sqrt{40}}\right)_i$ have the quantum numbers of Higgs doublets. Other components of these $SU(5)$ multiplets form color triplets of exotic quarks $\overline{D}_i$ and D_i with electric charges $-1/3$ and $+1/3$ respectively. However these

exotic quark states carry a $B-L$ charge $\left(\pm\frac{2}{3}\right)$ twice larger than that of ordinary ones. Therefore in the phenomenologically viable E_6 inspired models they can be either diquarks or leptoquarks.

In addition to the complete 27_i multiplets some components of the extra $27'$ and $\overline{27'}$ representations must survive to low energies in order to preserve gauge coupling unification. We assume that an additional $SU(2)$ doublet components H' of $\left(5^*,\,\frac{2}{\sqrt{40}}\right)$ from a $27'$ and corresponding anti-doublet $\overline{H}'$ from $\overline{27'}$ survive to low energies. Thus in addition to a Z' the E$_6$SSM involves extra matter beyond the MSSM that forms three $5+5^*$ representations of $SU(5)$ plus three $SU(5)$ singlets with $U(1)_N$ charges.

The superpotential in E_6 inspired models involves a lot of new Yukawa couplings in comparison to the SM. In general these new interactions induce non-diagonal flavour transitions. To suppress flavour changing processes one can postulate a Z_2^H symmetry under which all superfields except one pair of H_{1i} and H_{2i} (say $H_d \equiv H_{13}$ and $H_u \equiv H_{23}$) and one SM-type singlet field ($S \equiv S_3$) are odd. The Z_2^H symmetry reduces the structure of the Yukawa interactions to:

$$\begin{aligned} W_{\rm ESSM} \;\simeq\; & \lambda_i S(H_{1i}H_{2i}) + \kappa_i S(D_i\overline{D}_i) + f_{\alpha\beta}S_\alpha(H_dH_{2\beta}) + \tilde{f}_{\alpha\beta}S_\alpha(H_{1\beta}H_u) + \\ & + h_t(H_uQ)t^c + h_b(H_dQ)b^c + h_\tau(H_dL)\tau^c\,, \end{aligned} \tag{6.25}$$

where $\alpha,\beta = 1,2$ and $i = 1,2,3$. In Eq. (6.25) we keep only Yukawa interactions whose couplings are allowed to be of order unity and ignore H' and $\overline{H}'$ for simplicity. Here we define $h_s \equiv \lambda_3$. The $SU(2)$ doublets H_u and H_d play the role of Higgs fields generating the masses of quarks and leptons after EWSB. Therefore it is natural to assume that only S, H_u and H_d acquire non-zero VEVs. If h_s or κ_i are large at the grand unification (GUT) scale M_X they affect the evolution of the soft scalar mass m_S^2 of the singlet field S rather strongly resulting in negative values of m_S^2 at low energies that trigger the breakdown of the $U(1)_N$ symmetry. To guarantee that only H_u, H_d and S acquire a VEV we impose a certain hierarchy between the couplings H_{1i} and H_{2i} to the SM-type singlet superfields S_i: $h_s \gg \lambda_{1,2},\, f_{\alpha\beta}$ and $\tilde{f}_{\alpha\beta}$.

Although Z_2^H eliminates any problem related with non-diagonal flavour transitions it also forbids all Yukawa interactions that would allow the exotic quarks to decay. Since models with stable charged exotic particles are ruled out by different experiments [79] the Z_2^H symmetry must be broken. However even a small violation of this discrete symmetry permits to get a phenomenologically acceptable model. Because the Yukawa interactions of exotic particles to quarks and leptons of the first two generations give an appreciable contribution to the amplitude of $K^0-\overline{K}^0$ oscillations and give rise to new muon decay channels like $\mu \to e^-e^+e^-$ we assume that the violation of the Z_2^H symmetry in the E$_6$SSM is mainly caused by the Yukawa couplings of the exotic particles to the quarks and leptons of the third generations.

6.3.2 Higgs and collider phenomenology

The potential of the E$_6$SSM Higgs sector that involves two $SU(2)$ doublets H_u and H_d as well as the SM-type singlet field S is given by Eqs. (6.2)-(6.5) in the Introduction of this section. The value of the extra $U(1)_N$ gauge coupling $g_{Z'}$ appearing in the Higgs scalar potential can be determined assuming gauge coupling unification. It turns out that for any renormalisation scale Q below the unification scale ($Q < M_X$) $g_{Z'}(Q) \simeq \sqrt{\frac{5}{3}}g_1(Q)$, where $g_1(Q)$ is the $U(1)_Y$ gauge coupling ($g_1(M_Z) \simeq 0.36$) [28]. The only new coupling in the Higgs sector is then $h_sSH_dH_u$ which shows that the Higgs sector of the E$_6$SSM contains only one additional singlet field and one extra parameter compared to the MSSM. Therefore it can be regarded as the simplest extension of the Higgs sector of the MSSM.

At the physical vacuum Higgs fields develop the VEVs $\langle H_d\rangle = \frac{v_d}{\sqrt{2}}$, $\langle H_u\rangle = \frac{v_u}{\sqrt{2}}$ and $\langle S\rangle = \frac{s}{\sqrt{2}}$, thus breaking the $SU(2)_L \times U(1)_Y \times U(1)_N$ symmetry to $U(1)_{\rm EM}$, associated with electromagnetism. Instead of v_d and v_u it is more convenient to use $\tan\beta = \frac{v_u}{v_d}$ and $v = \sqrt{v_d^2+v_u^2}$, where $v = 246\,{\rm GeV}$. After the breakdown of the gauge symmetry two CP-odd and two charged Goldstone modes in the Higgs

sector are absorbed by the Z, Z' and $W^{\pm}$ gauge bosons so that only six physical degrees of freedom are left. They represent three CP-even (as in the NMSSM), one CP-odd and two charged Higgs states (as in the MSSM).

When the mass of the CP-odd Higgs boson m_{A^0} is considerably larger than M_Z the tree-level masses of the Higgs particles can be written as [28]

$$m^2_{A^0} \simeq m^2_{H^\pm} \simeq m^2_{h^0_3} \simeq \frac{2h_s^2 s^2 x}{\sin^2 2\beta}\,, \qquad\qquad m^2_{h^0_2} \simeq g^2_{Z'} Q^2_S s^2\,, \tag{6.26}$$

$$\begin{aligned} m^2_{h^0_1} \;\simeq\; & \frac{h_s^2}{2} v^2 \sin^2 2\beta + \frac{\bar{g}^2}{4} v^2 \cos^2 2\beta + g^2_{Z'} v^2 \Big(Q_{H_1} \cos^2\beta + Q_{H_2} \sin^2\beta \Big)^2 - \\ & - \frac{h_s^4 v^2}{g^2_{Z'} Q^2_S} \Big(1 - x + \frac{g^2_{Z'}}{h_s^2} \Big(Q_{H_1} \cos^2\beta + Q_{H_2} \sin^2\beta \Big) Q_S \Big)^2\,, \end{aligned} \tag{6.27}$$

where $m_{H^\pm}$ and $m_{h^0_i}$ are the masses of charged and CP-even states respectively while $x = \dfrac{A_h}{\sqrt{2} h_s s} \sin 2\beta$. From Eqs. (6.26)-(6.27) it follows that at tree level the Higgs spectrum can be parametrised in terms of four variables only: h_s, s, $\tan\beta$, m_{A^0} (or x). As one can see at least one CP-even Higgs boson is always heavy preventing the distinction between the E$_6$SSM and MSSM Higgs sectors. Indeed the mass of the singlet dominated Higgs scalar particle $m_{h^0_2}$ is always close to the mass of the Z' boson $M_{Z'} \simeq g_{Z'} Q_S s \sim g_{Z'} s$ that has to be heavier than $600 - 800\,\text{GeV}$. The masses of the charged, CP-odd and one CP-even Higgs states are governed by m_{A^0}. The mass of the SM-like Higgs boson given by Eq. (6.27) is set by M_Z. The last term in Eq. (6.27) must not be allowed to dominate since it is negative. This constrains x around unity for $h_s > g_{Z'}$. As a consequence m_{A^0} is confined in the vicinity of $\dfrac{h_s s}{\sqrt{2}} \tan\beta$ and is much larger than the masses of the Z' and Z bosons. At so large values of m_{A^0} the masses of the heaviest CP-even, CP-odd and charged states are almost degenerate around m_{A^0}.

The qualitative pattern of the Higgs spectrum obtained for $h_s > g_{Z'}$ is shown in Fig. 6.6 where we plot the masses of the Higgs bosons as a function of m_{A^0}. As a representative example we fix $\tan\beta = 2$ and the VEV of the singlet field $s = 1.9\,\text{TeV}$, corresponding to $M_{Z'} \simeq 700\,\text{GeV}$, which is quite close to the current limit on the Z' boson mass. For our numerical study we also choose the maximum possible value of $h_s(M_t) \simeq 0.794$ which does not spoil the validity of perturbation theory up to the GUT scale for $\tan\beta = 2$. In order to obtain a realistic spectrum, we include the leading one-loop corrections from the top and stop loops that depend rather strongly on the soft masses of the superpartners of the top-quark (m^2_Q and m^2_U) and on the stop mixing parameter X_t. Here and in the following we set $m_Q = m_U = M_S = 700\,\text{GeV}$ while X_t is taken to be $\sqrt{6}\, M_S$ in order to enhance stop-radiative effects.

The numerical analysis confirms the analytic tree-level results discussed above. From Fig. 6.6 it becomes clear that for m_{A^0} below 2 TeV or above 3 TeV the mass squared of the lightest Higgs boson tends to be negative. Negative value of $m^2_{h^0_1}$ implies that the considered vacuum configuration is unstable, i.e. there is a direction in field space along which the energy density decreases. The requirement of stability of the physical vacuum therefore limits the range of variations of m_{A^0} from below and above. Together with the experimental lower limit on the mass of the Z' boson it maintains the mass hierarchy in the spectrum of the Higgs particles seen in Fig. 6.6. The numerical analysis also reveals that the heaviest CP-even, CP-odd and charged Higgs states lie beyond the TeV range when $h_s > g_{Z'}$. The second lightest CP-even Higgs boson is predominantly singlet so that it will be quite difficult to observe at colliders.

When $h_s < g_{Z'}$ the allowed range of m_{A^0} enlarges. Although the requirement of vacuum stability still prevents having very high values of m_{A^0} (or x) the mass squared of the lightest Higgs boson remains positive even if charged, CP-odd and second lightest CP-even Higgs states lie in the $200-300\,\text{GeV}$ range. But for $m_{A^0} < 500\,\text{GeV}$ and $h_s < g_{Z'}$ we get an MSSM-type Higgs spectrum with the lightest SM-like Higgs boson below $130\,\text{GeV}$ and with the heaviest scalar above $600 - 800\,\text{GeV}$ being singlet dominated

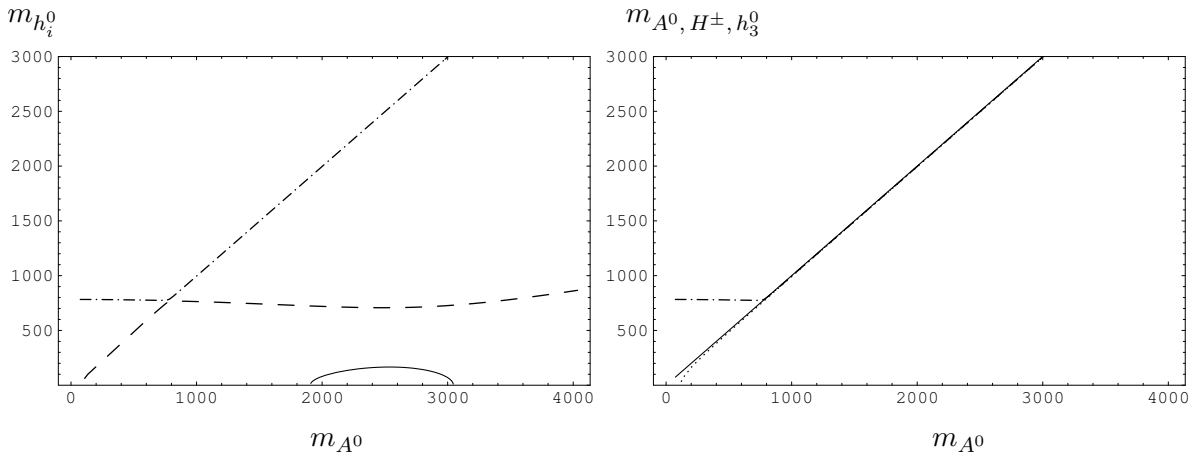

Fig. 6.6: Higgs masses for $h_s(M_t) = 0.794$, $\tan\beta = 2$, $M_{Z'} = M_S = 700\,\text{GeV}$ and $X_t = \sqrt{6}M_S$. Left: One-loop masses of the CP-even Higgs bosons versus m_{A^0}. Solid, dashed and dashed-dotted lines correspond to the masses of the lightest, second lightest and heaviest Higgs scalars respectively. Right: One-loop masses of the CP-odd, heaviest CP-even and charged Higgs bosons versus m_{A^0}. Dotted, dashed-dotted and solid lines correspond to the masses of the charged, heaviest scalar and pseudoscalar states.

and phenomenologically irrelevant. The non-observation of Higgs particles at LEP rules out most parts of the E_6SSM parameter space in this case.

From Fig. 6.6 and Eq. (6.27) it becomes clear that at some value of m_{A^0} (or x) the lightest CP-even Higgs boson mass $m_{h_1^0}$ attains its maximum value. At tree level the upper bound on $m_{h_1^0}$ is given by the sum of the first three terms in Eq. (6.27). The inclusion of loop corrections increases the bound on the lightest CP-even Higgs boson mass in models of supersymmetry (SUSY) substantially. When the soft masses of the superpartners of the top-quark are equal to M_S^2, the upper limit on $m_{h_1^0}$ in the E_6SSM in the leading two-loop approximation can be written in the following form [28]- [29]:

$$\begin{aligned} m^2_{h_1^0} \;\leq\; & \left[\frac{h_s^2}{2}v^2\sin^2 2\beta + M_Z^2\cos^2 2\beta + g_{Z'}^2 v^2\left(\tilde{Q}_1\cos^2\beta + \tilde{Q}_2\sin^2\beta\right)^2\right]\left(1 - \frac{3h_t^2}{8\pi^2}l\right) \\ + \;& \frac{3h_t^4 v^2\sin^4\beta}{8\pi^2}\left\{\frac{1}{2}U_t + l + \frac{1}{16\pi^2}\left(\frac{3}{2}h_t^2 - 8g_3^2\right)(U_t + l)l\right\}, \end{aligned} \tag{6.28}$$

where $U_t = 2\dfrac{X_t^2}{M_S^2}\left(1 - \dfrac{1}{12}\dfrac{X_t^2}{M_S^2}\right)$, $l = \ln\left[\dfrac{M_S^2}{m_t^2}\right]$. Eq. (6.28) is a simple generalisation of the approximate expressions for the two-loop theoretical restriction on the mass of the lightest Higgs particle obtained in the MSSM [80] and NMSSM [56]. If as before we assume that $M_S = 700\,\text{GeV}$ and $X_t = \sqrt{6}\,M_S$ then the theoretical restriction on the lightest Higgs mass given by Eq. (6.28) depends on h_s and $\tan\beta$ only. The requirement of validity of perturbation theory up to the GUT scale constrains the parameter space further setting a limit on the Yukawa coupling $h_s(M_t)$ for each value of $\tan\beta$. Relying on the results of the analysis of the renormalisation group flow in the E_6SSM presented in [28] one can obtain the maximum possible value of the lightest Higgs scalar for each particular choice of $\tan\beta$.

The dependence of the tree-level and two-loop upper bounds on the mass of the lightest Higgs particle is examined in Fig. 6.7 where it is compared with the corresponding limits in the MSSM and NMSSM. At moderate values of $\tan\beta$ $(1.6 - 3.5)$ the upper limit on the lightest Higgs boson mass in the E_6SSM is considerably higher than in the MSSM and NMSSM. In the leading two-loop approximation it reaches the maximum value $150 - 155\,\text{GeV}$ at $\tan\beta = 1.5 - 2$ [28]- [29]. Remarkably, we find that in the interval of $\tan\beta$ from 1.2 to 3.4 the absolute maximum value of the mass of the lightest Higgs scalar in the E_6SSM is larger than the experimental lower limit on the SM-like Higgs boson even at tree level. Therefore the non-observation of Higgs bosons at LEP does not cause any trouble for the E_6SSM.

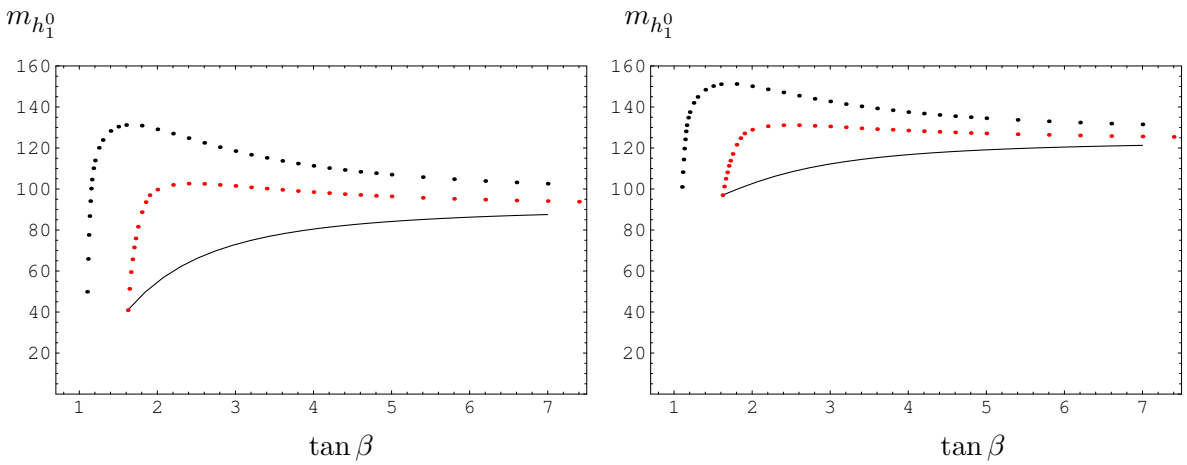

Fig. 6.7: Upper bound on the mass of the lightest Higgs boson. The solid, lower and upper dotted lines correspond to the theoretical restrictions on the lightest Higgs mass in the MSSM, NMSSM and E_6SSM respectively. Left: tree-level upper limit on the mass of the lightest Higgs particle as a function of $\tan\beta$. Right: Two-loop upper bound on the lightest Higgs mass versus $\tan\beta$.

In the considered part of the parameter space the theoretical restriction on the mass of the lightest CP-even Higgs boson in the NMSSM exceeds the corresponding limit in the MSSM because of the extra contribution to $m^2_{h^0_1}$ induced by the additional F-term in the Higgs scalar potential of the NMSSM. The size of this contribution, which is described by the first term in Eq. (6.27), is determined by the Yukawa coupling h_s. The upper limit on h_s caused by the validity of perturbation theory in the NMSSM is more stringent than in the E_6SSM. Indeed new exotic $5+\overline{5}$-plets of matter in the particle spectrum of the E_6SSM change the running of the gauge couplings so that their values at the intermediate scale rise preventing the appearance of the Landau pole in the evolution of the Yukawa couplings. It means that for each value of $\tan\beta$ the maximum allowed value of $h_s(M_t)$ in the E_6SSM is larger than in the NMSSM. The increase of $h_s(M_t)$ is accompanied by the growth of the theoretical restriction on the mass of the lightest CP-even Higgs particle. This is the main reason why the upper bound on $m_{h^0_1}$ in the E_6SSM exceeds that in the NMSSM.

At large $\tan\beta > 10$ the contribution of the F-term of the SM-type singlet field to $m^2_{h^0_1}$ vanishes. Therefore with increasing $\tan\beta$ the upper bound on the lightest Higgs boson mass in the NMSSM approaches the corresponding limit in the MSSM. In the E_6SSM the theoretical restriction on the mass of the lightest Higgs scalar also diminishes when $\tan\beta$ rises. But even at very large values of $\tan\beta$ the two-loop upper limit on $m_{h^0_1}$ in the E_6SSM is still $4-5\,\text{GeV}$ larger than the ones in the MSSM and NMSSM because of the $U(1)_N$ D-term contribution to $m_{h^0_1}$ (the third term in Eq. (6.27)). This contribution is especially important in the case of minimal mixing between the superpartners of the top quark. In the considered case the two-loop theoretical restriction on $m_{h^0_1}$ in the MSSM and NMSSM is less than the experimental limit on the SM-like Higgs boson mass set by LEP. As a result the scenario with $X_t = 0$ is ruled out in the MSSM. The contribution of an extra $U(1)_N$ D-term to $m^2_{h^0_1}$ raises the upper bound given by Eq. (6.28) at large $\tan\beta \geq 10$ slightly above the existing LEP limit thus relaxing the constraints on the E_6SSM parameter space. The discovery at future colliders of a relatively heavy SM-like Higgs boson with mass $140-155\,\text{GeV}$, corresponding to $h_s > g_{Z'}$ in the E_6SSM, will permit to distinguish the E_6SSM from the MSSM and NMSSM.

Other possible manifestations of our exceptional SUSY model at the LHC are related to the presence of a Z' and of exotic multiplets of matter. For instance, a relatively light Z' will lead to enhanced production of l^+l^- pairs ($l = e, \mu$). The analysis performed in [81] revealed that a Z' boson in E_6 inspired models can be discovered at the LHC if its mass is less than $4-4.5\,\text{TeV}$. At the same time the

determination of its couplings should be possible up to $M_{Z'} \sim 2-2.5$ TeV [82]. Moreover in the E$_6$SSM the exotic fermions can be relatively light since their masses are set by the Yukawa couplings κ_i and λ_i that may be small. This happens, for example, when the Yukawa couplings of the exotic particles have a hierarchical structure which is similar to the one observed in the ordinary quark and lepton sectors. Then the production cross section of exotic quark pairs at the LHC can be comparable with the cross section of $t\bar{t}$ production. The lifetime of new exotic particles is defined by the extent to which the Z_2^H symmetry is broken. Since we have assumed that Z_2^H is mainly broken by operators involving quarks and leptons of the third generation the lightest exotic quarks decay into either two heavy quarks $Q\bar{Q}$ or a heavy quark and a lepton $Q\tau(\nu_\tau)$, where Q is either a b- or t-quark. In the case when Z_2^H is broken significantly this results in the growth of the cross section of either $pp \to Q\bar{Q}Q^{(\prime)}\bar{Q}^{(\prime)} + X$ or $pp \to Q\bar{Q}l^+l^- + X$. If the violation of the Z_2^H invariance is extremely small then a set of new composite scalar leptons or baryons containing quasi-stable exotic quarks could be discovered at the LHC. The discovery of the Z' and exotic quarks predicted by the E$_6$SSM would represent a possible indirect signature of an underlying E_6 gauge structure at high energies and provide a window into string theory.

6.4 Doubly charged Higgs bosons from the left-right symmetric model at the LHC

Georges Azuelos, Kamal Benslama and Jonathan Ferland

The Left-Right Symmetric Model (LRSM) [83–85], based on the group $SU(2)_L \otimes SU(2)_R \otimes U(1)_{B-L}$, is a natural extension of the Standard Model, deriving from Grand Unified Theories. The breaking of $SU(2)_R \otimes U(1)_{B-L} \to U(1)_Y$ occurs at a high energy scale due to a triplet of complex Higgs fields[2] with physical states consisting of Δ_R^0, Δ_R^+ and Δ_R^{++}, when the neutral component acquires a non-vanishing vacuum expectation value (An overview of triplet models is given in Section 13.1). The Higgs sector of the model therefore contains a doubly charged Higgs boson, which could provide a clean signature at the LHC since charge conservation prevents it from decaying to a pair of quarks. Doubly charged scalars are also predicted in Little Higgs models [89, 90], see Section 7, and in 3-3-1 models [91–94], where doubly charged vector bilepton states are also predicted. Very light, $\mathcal{O}(\sim 100)$ GeV, doubly-charged Higgs particles can also be expected in supersymmetric left-right models [36, 95]. Here, we summarize the results [46] of an analysis, performed for ATLAS, which expands on previous phenomenological studies [39,96–98] by including the effects of backgrounds as well as detector acceptance and resolution.

Other signatures involving the decay of the new heavy gauge bosons of the LRSM have been studied in ATLAS [99–102]. As a complement to these searches, observation of a doubly charged Higgs would clearly provide an important confirmation of the nature of the new physics. In fact, heavy gauge bosons could be out of kinematical reach, and the Majorana neutrinos could be extremely heavy ($\sim 10^{11}$ GeV) if the see-saw mechanism explains the mass of the light neutrinos. Thus the observation of a doubly-charged Higgs boson could serve as the discovery channel for the LRSM.

The Higgs sector [39] of the LRSM consists of (i) the right-handed complex triplet Δ_R mentioned above, with weights (0,1,2), meaning singlet in $SU(2)_L$, triplet in $SU(2)_R$ and $B - L = 2$, (ii) a left-handed triplet Δ_L (1,0,2) (if the Lagrangian is to be symmetric under $L \leftrightarrow R$ transformation); and a bidoublet ϕ (1/2,1/2,0). The vacuum expectation values (vev) of the neutral members of the scalar triplets, v_L and v_R, break the symmetry $SU(2)_L \times SU(2)_R \times U(1)_{B-L} \to SU(2)_L \times U(1)_Y$. The non-vanishing vev of the bidoublet breaks the SM $SU(2)_L \times U(1)_Y$ symmetry. It is characterized by two parameters κ_1 and κ_2, with $\kappa = \sqrt{\kappa_1^2 + \kappa_2^2} = 246$ GeV. To prevent flavour changing neutral currents (FCNC), one must have $\kappa_2 \ll \kappa_1$, implying minimal mixing between W_L and W_R [103]. The mass eigenstate of the singly charged Higgs is a mixed state of the charged components of the bidoublet and of the triplet. Bounds on the parameters are given in [39, 98, 104]: custodial symmetry constrains $v_L \lesssim 9$ GeV and present Tevatron lower bounds on M_{W_R} impose a limit $v_R > 1.4$ TeV, or

[2] Alternative minimal Left-Right symmetric models exist with only doublets of scalar fields [86–88]. They do not lead to Majorana couplings of the right-handed neutrinos.

$m_{W_R} > 650$ GeV, assuming equal gauge couplings $g_L = g_R$. Direct limits from the Tevatron on the mass of the doubly charged Higgs from di-leptonic decays have recently been reported in [105, 106]. Indirect limits on the mass and couplings of the triplet Higgs bosons, obtained from various processes, are given in [39, 104, 107] (see also Section 13).

We will assume a truly symmetric Left-Right model, with equal gauge couplings $g_L = g_R = e/\sin(\theta_W) = 0.64$. We relate the mass of W_R to v_R by: $m^2_{W_R} = g^2_R v^2_R/2$, which is a valid approximation in the limit where $v_L = 0$ and $\kappa_1 \ll v_R$.

6.4.1 Phenomenology of the doubly-charged Higgs boson

Single production of Δ^{++}_R production is dominated by the vector fusion process $W^{\pm}_R W^{\pm}_R$, as long as the mass of the W_R is of the TeV scale [98]. For the process $W^+W^+ \to \Delta^{++}_L$, the suppression due to the small value of the v_L is somewhat compensated by the fact that the incoming quarks radiate a lower mass vector gauge boson.

Double production of the doubly charged Higgs is also possible via a Drell-Yan process, with γ, Z or Z_R exchanged in the s-channel, but at a high kinematic price since enough energy is required to produce two heavy particles. In the case of Δ^{++}_L, double production may nevertheless be the only possibility if v_L is very small or vanishing.

The decay of a doubly charged Higgs can proceed by several channels. Present bounds [98, 107] on the diagonal couplings $h_{ee,\mu\mu,\tau\tau}$ to charged leptons are consistent with values $\sim O(1)$ if the mass scale of the triplet is larger than a few hundred GeV. For the Δ^{++}_L, this may be the dominant coupling if v_L is very small. For very low Yukawa couplings ($h_{\ell\ell} \lesssim 10^{-8}$), the doubly charged Higgs boson could be quasi-stable [108], leaving a characteristic dE/dx signature in the detector, but this case is not considered here. The decay $\Delta^{++}_{R,L} \to W^+_{R,L} W^+_{R,L}$ can also be significant. However, it is kinematically suppressed in the case of Δ^{++}_R, and suppressed by the small coupling v_L in the case of Δ^{++}_L.

Here, we discuss only dilepton (ee or $\mu\mu$) decay, which provides a clean signature, kinematically enhanced, although the branching ratios will depend on the unknown Yukawa couplings. A complete description of this analysis as well as of other channels, including $\tau\tau$ and WW can be found in [46].

6.4.2 Simulation of the signal and backgrounds

The processes of single and double production of doubly charged Higgs are implemented in the PYTHIA generator [109]. Events were generated using the CTEQ5L parton distribution functions, taking account of initial and final state interactions as well as hadronization.

Detector effects and acceptance were simulated using ATLFAST [110], a fast simulation program for the ATLAS detector, where efficiencies and resolutions are parametrized according to the expected detector performance, as evaluated in [99].

PYTHIA was used to generate the $t\bar{t}$ background, which has a very large cross section of ~ 500 pb. Other backgrounds were simulated using the CompHep generator [111]: (i) The Standard Model processes $qq \to W^+W^+qq$ and (ii) $qq \to W^+Zqq$ and (iii) $pp \to Wt\bar{t}$.

A number of systematic uncertainties, some of which are difficult to evaluate reliably before experimental data are available, will apply. No k-factors have been used here, although next-to-leading-order corrections can be substantial for these high mass resonance states. Experimental systematic uncertainties involve: the luminosity measurement ($\sim 5 - 10\%$), the efficiency of lepton reconstruction in ATLAS, here taken to be 90%, the uncertainty in the energy resolution, especially for high energy electrons, charge misidentification, estimated to be small, and misidentification of jets as electrons, for which preliminary estimates suggest that it will have a small effect.

Table 6.1: Number of events of signal and backgrounds after successive application of cuts, for the case $\Delta_R^{++} \to \ell^+ \ell^+$, around $m_{\ell\ell}$ = 300 or 800 GeV (shown as n_{300}/n_{800} for the backgrounds), for m_{W_R} = 650 GeV and for 100 fb^{-1}. Mass windows $\pm 2\sigma$ around the resonances have been chosen. In parentheses is shown the number of events without the mass window cut.

	Δ^{++} 300 GeV	Δ^{++} 800 GeV	$W^+W^+\,qq$	$W\,t\bar{t}$	$WZqq$	$t\bar{t}$	total backg
Isolated leptons	278 (327)	63 (95)	109/12	7.6/0.6	0/0.8	17/0	133/13
Lepton $P_T > 50$ GeV	256 (301)	63 (94)	63/11	5.9/0.5	0/0.8	1.1/0	70/12
$2.4(P_T^{l_1} + P_T^{l_2}) - M_{ll} > 480$	191(227)	59(85)	10/2.1	1.3/0.3	0	0	12/2.4
Fwd Jet tagging	156(186)	56(74)	6.0/1.3	0.1/0	0	0	6/1.3
ptmiss $<$ 100 GeV	154(181)	56(68)	3.0/0.3	0/0	0	0	3.1/0.3

6.4.3 Search for $\boldsymbol{\Delta_R^{++}}$

The cross section for single production of Δ_R^{++} is of the order of $\sim$ fb: for example, it is 0.9 fb for the case $m(\Delta_R^{++}) = 800$ GeV, $m(W_R^{++}) = 850$ GeV. We consider signals for doubly positively charged Higgs bosons, as they are about 1.6 times more abundant than the negatively charged ones, at the LHC. The same ratio of positively charged to negatively charged leptons can be expected from the backgrounds, to the extent that $qqWW$ dominates, and hence the improvement in the significances obtained below can be estimated at 22%.

The selection criteria for this channel are summarized in Table 6.1, which also shows the number of events of signal for typical cases of signal where $m_{\Delta_R^{++}}$ = 300 or 800 GeV and $m_{W_R^+} = 650$ GeV, and of the various backgrounds after successive application of cuts. A clean signal is found for an integrated luminosity of 100 fb^{-1}. A window of $\pm 2\times$ the width of the reconstructed mass of the Δ_R^{++} has been selected. The intrinsic width depends on the assumed $\Delta_R^{++} - \ell\ell$ couplings, but is expected, in any case to be very narrow [98]. The width is therefore dominated by the detector resolution, which is measured to be $\sigma_R = 20$, 55 and 123 GeV for the cases of Δ_R^{++}= 300, 800, 1500 GeV respectively. The cuts involve forward jet tagging (for details, see [46]), since the primary partons from which the W_R are radiated will tend to continue in the forward and background directions, and hadronize as jets.

Since the background is negligible, discovery can be claimed if the number of signal events is 10 or higher. With this definition, the contour of discovery, in the plane $m_{W_R^+}$ versus $m_{\Delta_R^{++}}$ (or v_R) has been estimated from a sample of test cases. The discovery reach at the LHC is shown in Fig. 6.8, for integrated luminosities of 100 fb^{-1} and 300 fb^{-1} and assuming 100% BR to lepton pairs.

Pair production of $\Delta_R^{++}\Delta_R^{--}$ is suppressed by the expected high mass of the Δ_R^{++} but can have a dominant cross section in some region of phase space (see [98]). The diagrams with s-channel Z and Z' exchange have been added to the γ exchange diagram in the implementation of the Drell-Yan process in the PYTHIAg generator, taking the coupling of Z, Z' to fermions and to Δ_L^{++} from references [96, 112]. In principle, the branching ratio depends on the assumed mass of Δ_L^{++}, as well as that of Δ_R^{++}, but since the Z' has a large partial width to fermions, such that $BR(Z' \to \Delta^{++}\Delta^{--})$ is of the order of 1%, the contribution of these decay channels to the total width of the Z' was neglected. For the case of leptonic decays of the doubly-charged Higgs bosons, the process constitutes a golden channel and the background will be negligible.

Fig. 6.9 shows the contours of discovery, defined as observation of 10 events, if all four leptons are detected or if any 3 of the leptons are observed. As $m(Z_R)$ increases, the mass reach for $m(\Delta_R^{++})$ increases at first, as the s-channel diagram with Z_R produced on mass shell becomes the dominant contribution. However, for very large masses of Z_R, the contribution of this diagram is kinematically suppressed. Being an s-channel process not involving the W_R, this channel is not sensitive to the mass of this heavy gauge boson.

Table 6.2: Number of events of signal and total background after successive application of cuts, for the case $\Delta^{++} \to \ell^+ \ell^+$, for $m_{\Delta_L^{++}}$ = 300 or 800 GeV (shown as n_{300}/n_{800} for the background) and $v_L = 9$ GeV, for 100 fb^{-1}. Mass windows $\pm 2\sigma$ around the resonances have been chosen. In parentheses is shown the number of events without the mass window cut.

	Δ^{++} 300 GeV	Δ^{++} 800 GeV	total backg
Isolated leptons	330 (384)	59 (69)	133/13
$\|\Delta\phi_{\ell\ell} > 2.5\|$	253 (289)	56 (65)	75/8.3
$\Delta_{P_T^{ll}} > (\frac{M_{ll}}{2}$+50)	220 (260)	50 (59)	37/2.5
Fwd Jet tagging	144(170)	38 (45)	11/0.6
ptmiss	140(165)	33 (38)	2.0/0.07

6.4.4 Search for $\boldsymbol{\Delta_L^{++}}$

The search for Δ_L^{++} follows closely the strategy used for Δ_R^{++}. However, some major differences in the kinematics of the events force the use of different selection criteria. In particular, Δ_L^{++} single production occurs via fusion of a pair of W_L's, which are much lighter than the W_R's in the case of single production of Δ_R^{++}. The distribution of forward jets is strongly affected, as well as the final transverse momentum of the Δ^{++}. For that reason, an independent analysis has been performed, using cuts similar to the case of Δ_R^{++} to the extent possible (for details, see [46]).

As for the case of the Δ_R^{++} the dilepton channel provides a clean signature. Although the Yukawa coupling of Δ_L^{++} to leptons remains a parameter of the theory, this channel can, in fact, be dominant since the alternative decay to gauge bosons is possibly negligible, being proportional to the very small value of the vev v_L. In the limit where $v_L = 0$, it will be the only open channel, but production of Δ_L^{++} will only occur in pairs, through s-channel $\gamma/Z/Z'$ exchange. As before, we will assume below 100% branching ratio to leptons, but results can be reinterpreted in a straightforward way for different values of this branching ratio.

Table 6.2 gives the number of expected signal and background events for the cases $m_{\Delta_L^{++}} = 300$ GeV and $m_{\Delta_L^{++}} = 800$ GeV respectively. A mass window of $\pm 2\times$ the width of the resonance was selected. The discovery reach in the plane v_L vs $m_{\Delta_L^{++}}$ is shown in Fig. 6.10.

As for the case of the right-handed sector, pair production of Δ_L is a possible discovery channel. The diagram with s-channel Z' exchange has been added to the implementation of this Drell-Yan process in the PYTHIA generator, taking the coupling of Z' to fermions and to Δ_L^{++} from references [96, 112]. Assuming leptonic decays, the background will be negligible. Fig. 6.11 shows the contours of discovery, defined as observation of 10 events, if all four leptons are detected or if at least any 3 of the leptons are observed. The reach has the same qualitative dependence on the mass of Z_R as for the case of Δ_R^{++} pair production.

6.4.5 Summary and Conclusion

Left-Right symmetric models predict the existence of doubly-charged Higgs bosons which should yield a striking signature at the LHC. The principal production and decay modes, including $\Delta \to \tau\tau$ and $\Delta \to WW$ have been investigated in [46] but only the dilepton channel is reported here. It must be emphasized that these results have assumed that the decay to two leptons (e or μ) dominate and that they should be rescaled if there is a substantial branching ratio to $\tau\tau$. It is found that the LHC will be able to probe a large region of unexplored parameter space in the triplet Higgs sector. This analysis complements previous ATLAS studies searching for signals of the Left-Right symmetric model.

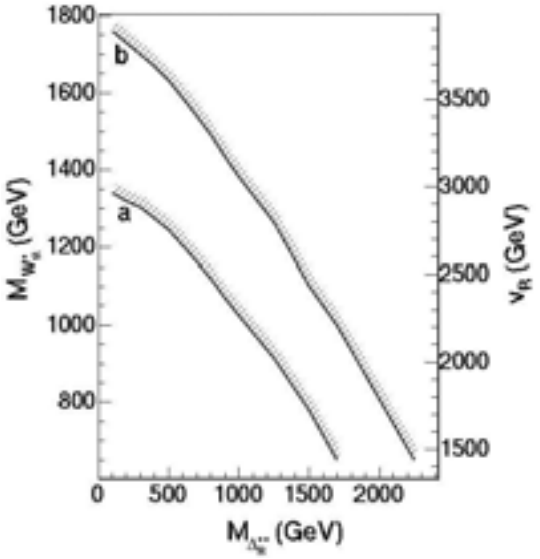

Fig. 6.8: Discovery reach for $\Delta_R^{++} \to l^+l^+$ in the plane $m_{W_R^+}$ versus $m_{\Delta_R^{++}}$ (or v_R) for integrated luminosities of 100 fb^{-1}(a) and 300 fb^{-1}(b), and assuming 100% BR to dileptons. The region where discovery is not possible is on the hatched side of the line.

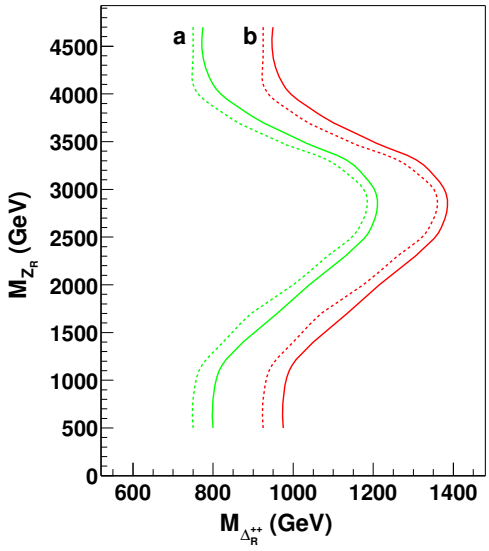

Fig. 6.9: Contours of discovery for 100 fb^{-1}(a) and for 300 fb^{-1}(b) in the plane $m_{Z'}$ vs $m_{\Delta_R^{++}}$. The dashed curves are for the case where all four leptons are observed, and the full curves are when only three leptons are detected.

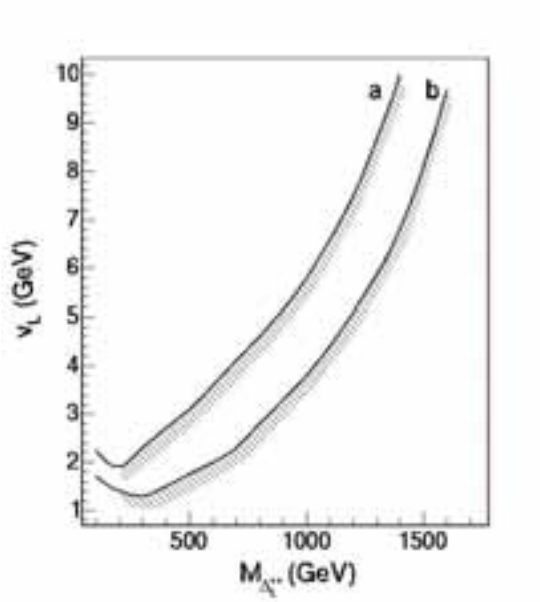

Fig. 6.10: Discovery reach for $\Delta_L^{++} \to \ell^+\ell^+$ in the plane v_L versus $m_{\Delta_L^{++}}$ for integrated luminosities of 100 fb^{-1}(a) and 300 fb^{-1}(b) and assuming 100% BR to dileptons.

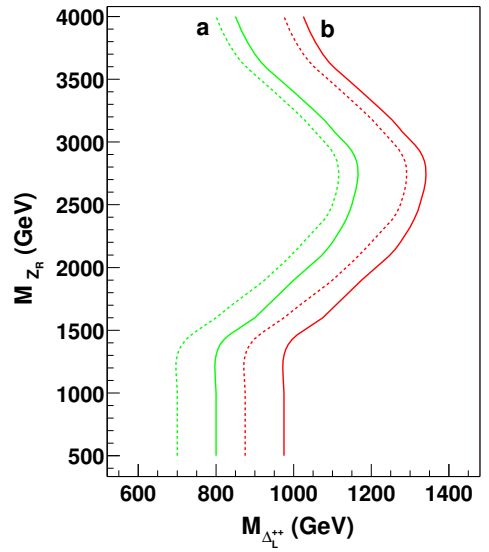

Fig. 6.11: Contours of discovery in the plane $m_{Z'}$ vs $m_{\Delta_L^{++}}$ for 100 fb^{-1}(a) and 300 fb^{-1}(b). The dashed curves are for the case where all four leptons are observed, and the full curves are when only three leptons are detected.

REFERENCES

[1] R. N. Mohapatra, Unification and Supersymmetry: The Frontiers of Quark–Lepton Physics, 3rd ed., (Springer, Berlin, 2003).

[2] M. Cvetic and P. Langacker, Phys. Rev. **D54**, 3570 (1996), [hep-ph/9511378].

[3] M. Cvetic and P. Langacker, hep-ph/9707451.

[4] T. Han, H. E. Logan, B. McElrath and L.-T. Wang, Phys. Rev. **D67**, 095004 (2003), [hep-ph/0301040].

[5] M. Masip and A. Pomarol, Phys. Rev. **D60**, 096005 (1999), [hep-ph/9902467].

[6] C. T. Hill and E. H. Simmons, Phys. Rep. **381**, 235 (2003), [hep-ph/0203079].

[7] V. Barger, P. Langacker and H.-S. Lee, Phys. Lett. **B630**, 85 (2005), [hep-ph/0508027].

[8] V. Barger, P. Langacker and H.-S. Lee, AIP Conf. Proc. **805**, 306 (2006), [hep-ph/0509112].

[9] D. A. Demir and L. L. Everett, Phys. Rev. **D69**, 015008 (2004), [hep-ph/0306240].

[10] J. Kang, P. Langacker, T.-j. Li and T. Liu, Phys. Rev. Lett. **94**, 061801 (2005), [hep-ph/0402086].

[11] J. Erler, Nucl. Phys. **B586**, 73 (2000), [hep-ph/0006051].

[12] D. Atwood, L. Reina and A. Soni, Phys. Rev. **D55**, 3156 (1997), [hep-ph/9609279].

[13] P. Langacker and M. Plumacher, Phys. Rev. **D62**, 013006 (2000), [hep-ph/0001204].

[14] H. E. Haber and M. Sher, Phys. Rev. **D35**, 2206 (1987).

[15] M. Drees, Phys. Rev. **D35**, 2910 (1987).

[16] J. F. Gunion, L. Roszkowski and H. E. Haber, Phys. Rev. **D38**, 105 (1988).

[17] J. R. Espinosa and M. Quiros, Phys. Lett. **B302**, 51 (1993), [hep-ph/9212305].

[18] G. L. Kane, C. F. Kolda and J. D. Wells, Phys. Rev. Lett. **70**, 2686 (1993), [hep-ph/9210242].

[19] D. Comelli and C. Verzegnassi, Phys. Lett. **B303**, 277 (1993).

[20] Y. Kawamura and M. Tanaka, Prog. Theor. Phys. **91**, 949 (1994).

[21] C. F. Kolda and S. P. Martin, Phys. Rev. **D53**, 3871 (1996), [hep-ph/9503445].

[22] M. Cvetic, D. A. Demir, J. R. Espinosa, L. L. Everett and P. Langacker, Phys. Rev. **D56**, 2861 (1997), [hep-ph/9703317].

[23] D. A. Demir, Phys. Rev. **D59**, 015002 (1999), [hep-ph/9809358].

[24] Y. Daikoku and D. Suematsu, Phys. Rev. **D62**, 095006 (2000), [hep-ph/0003205].

[25] S. Nie and M. Sher, Phys. Rev. **D64**, 073015 (2001), [hep-ph/0102139].

[26] H. Amini, New J. Phys. **5**, 49 (2003), [hep-ph/0210086].

[27] P. Langacker and J. Wang, Phys. Rev. **D58**, 115010 (1998), [hep-ph/9804428].

[28] S. F. King, S. Moretti and R. Nevzorov, Phys. Rev. **D73**, 035009 (2006), [hep-ph/0510419].

[29] S. F. King, S. Moretti and R. Nevzorov, Phys. Lett. **B634**, 278 (2006), [hep-ph/0511256].

[30] V. Barger, P. Langacker, H.-S. Lee and G. Shaughnessy, hep-ph/0603247.

[31] J. Erler, P. Langacker and T.-j. Li, Phys. Rev. **D66**, 015002 (2002), [hep-ph/0205001].

[32] T. Han, P. Langacker and B. McElrath, Phys. Rev. **D70**, 115006 (2004), [hep-ph/0405244].

[33] T. Han, P. Langacker and B. McElrath, hep-ph/0402064.

[34] D. Chang, R. N. Mohapatra and M. K. Parida, Phys. Rev. **D30**, 1052 (1984).

[35] D. Chang, R. N. Mohapatra and M. K. Parida, Phys. Rev. Lett. **52**, 1072 (1984).

[36] Z. Chacko and R. N. Mohapatra, Phys. Rev. **D58**, 015003 (1998), [hep-ph/9712359].

[37] G. C. Branco and L. Lavoura, Phys. Lett. **B165**, 327 (1985).

[38] J. Basecq, J. Liu, J. Milutinovic and L. Wolfenstein, Nucl. Phys. **B272**, 145 (1986).

[39] J. F. Gunion, J. Grifols, A. Mendez, B. Kayser and F. I. Olness, Phys. Rev. **D40**, 1546 (1989).

[40] N. G. Deshpande, J. F. Gunion, B. Kayser and F. I. Olness, Phys. Rev. **D44**, 837 (1991).

[41] J. Gluza and M. Zralek, Phys. Rev. **D51**, 4695 (1995), [hep-ph/9409225].
[42] G. Barenboim, M. Gorbahn, U. Nierste and M. Raidal, Phys. Rev. **D65**, 095003 (2002), [hep-ph/0107121].
[43] Y. Rodriguez and C. Quimbay, Nucl. Phys. **B637**, 219 (2002), [hep-ph/0203178].
[44] K. Kiers, M. Assis and A. A. Petrov, Phys. Rev. **D71**, 115015 (2005), [hep-ph/0503115].
[45] P. Herczeg and R. N. Mohapatra, Phys. Rev. Lett. **69**, 2475 (1992).
[46] G. Azuelos, K. Benslama and J. Ferland, J. Phys. **G32**, 73 (2006), [hep-ph/0503096].
[47] M. Schumacher, LC-PHSM-2003-096.
[48] A. Abulencia *et al.* (CDF Collaboration), hep-ex/0602045.
[49] ALEPH, DELPHI, L3 and OPAL Collaborations and the LEP Electroweak Working Group, hep-ex/0511027.
[50] J. Erler and P. Langacker, Phys. Lett. **B456**, 68 (1999), [hep-ph/9903476].
[51] J. Erler and P. Langacker, Phys. Rev. Lett. **84**, 212 (2000), [hep-ph/9910315].
[52] P. Langacker, N. Polonsky and J. Wang, Phys. Rev. **D60**, 115005 (1999), [hep-ph/9905252].
[53] M. Quiros and J. R. Espinosa, hep-ph/9809269.
[54] U. Ellwanger and M. Lindner, Phys. Lett. **B301**, 365 (1993), [hep-ph/9211249].
[55] U. Ellwanger and C. Hugonie, hep-ph/0006222.
[56] U. Ellwanger and C. Hugonie, Eur. Phys. J. **C25**, 297 (2002), [hep-ph/9909260].
[57] J. R. Ellis, J. F. Gunion, H. E. Haber, L. Roszkowski and F. Zwirner, Phys. Rev. **D39**, 844 (1989).
[58] H. P. Nilles, M. Srednicki and D. Wyler, Phys. Lett. **B120**, 346 (1983).
[59] M. Drees, Int. J. Mod. Phys. **A4**, 3635 (1989).
[60] U. Ellwanger and M. Rausch de Traubenberg, Z. Phys. **C53**, 521 (1992).
[61] P. N. Pandita, Z. Phys. **C59**, 575 (1993).
[62] P. N. Pandita, Phys. Lett. **B318**, 338 (1993).
[63] T. Elliott, S. F. King and P. L. White, Phys. Rev. **D49**, 2435 (1994), [hep-ph/9308309].
[64] R. Dermisek and J. F. Gunion, Phys. Rev. Lett. **95**, 041801 (2005), [hep-ph/0502105].
[65] R. Dermisek and J. F. Gunion, hep-ph/0510322.
[66] J. F. Gunion, D. Hooper and B. McElrath, Phys. Rev. **D73**, 015011 (2006), [hep-ph/0509024].
[67] S. Ambrosanio and B. Mele, Phys. Rev. **D53**, 2541 (1996), [hep-ph/9508237].
[68] J. F. Gunion, T. Han and R. Sobey, Phys. Lett. **B429**, 79 (1998), [hep-ph/9801317].
[69] U. Ellwanger, J. F. Gunion, C. Hugonie and S. Moretti, hep-ph/0305109.
[70] U. Ellwanger, J. F. Gunion and C. Hugonie, hep-ph/0111179.
[71] Y. Hosotani, Phys. Lett. **B129**, 193 (1983).
[72] J.-h. Kang, P. Langacker and T.-j. Li, Phys. Rev. **D71**, 015012 (2005), [hep-ph/0411404].
[73] E. Ma, Phys. Lett. **B380**, 286 (1996), [hep-ph/9507348].
[74] T. Hambye, E. Ma, M. Raidal and U. Sarkar, Phys. Lett. **B512**, 373 (2001), [hep-ph/0011197].
[75] E. Ma and M. Raidal, J. Phys. **G28**, 95 (2002), [hep-ph/0012366].
[76] E. Keith and E. Ma, Phys. Rev. **D54**, 3587 (1996), [hep-ph/9603353].
[77] D. Suematsu, Phys. Rev. **D57**, 1738 (1998), [hep-ph/9708413].
[78] E. Keith and E. Ma, Phys. Rev. **D56**, 7155 (1997), [hep-ph/9704441].
[79] T. K. Hemmick *et al.*, Phys. Rev. **D41**, 2074 (1990).
[80] M. Carena, M. Quiros and C. E. M. Wagner, Nucl. Phys. **B461**, 407 (1996), [hep-ph/9508343].
[81] J. Kang and P. Langacker, Phys. Rev. **D71**, 035014 (2005), [hep-ph/0412190].
[82] M. Dittmar, A.-S. Nicollerat and A. Djouadi, Phys. Lett. **B583**, 111 (2004), [hep-ph/0307020].

[83] R. N. Mohapatra and J. C. Pati, Phys. Rev. **D11**, 566 (1975).
[84] R. N. Mohapatra and J. C. Pati, Phys. Rev. **D11**, 2558 (1975).
[85] G. Senjanovic and R. N. Mohapatra, Phys. Rev. **D12**, 1502 (1975).
[86] K. S. Babu and R. N. Mohapatra, Phys. Rev. **D41**, 1286 (1990).
[87] Y. A. Coutinho, J. A. Martins Simoes and C. M. Porto, Eur. Phys. J. **C18**, 779 (2001), [hep-ph/0003296].
[88] B. Brahmachari, E. Ma and U. Sarkar, Phys. Rev. Lett. **91**, 011801 (2003), [hep-ph/0301041].
[89] N. Arkani-Hamed, A. G. Cohen and H. Georgi, JHEP **07**, 020 (2002), [hep-th/0109082].
[90] N. Arkani-Hamed, A. G. Cohen and H. Georgi, Phys. Lett. **B513**, 232 (2001), [hep-ph/0105239].
[91] F. Pisano and V. Pleitez, Phys. Rev. **D46**, 410 (1992), [hep-ph/9206242].
[92] R. Foot, O. F. Hernandez, F. Pisano and V. Pleitez, Phys. Rev. **D47**, 4158 (1993), [hep-ph/9207264].
[93] B. Dion, T. Gregoire, D. London, L. Marleau and H. Nadeau, Phys. Rev. **D59**, 075006 (1999), [hep-ph/9810534].
[94] F. Cuypers and S. Davidson, Eur. Phys. J. **C2**, 503 (1998), [hep-ph/9609487].
[95] C. S. Aulakh, A. Melfo and G. Senjanovic, Phys. Rev. **D57**, 4174 (1998), [hep-ph/9707256].
[96] J. A. Grifols, A. Mendez and G. A. Schuler, Mod. Phys. Lett. **A4**, 1485 (1989).
[97] R. Vega and D. A. Dicus, Nucl. Phys. **B329**, 533 (1990).
[98] K. Huitu, J. Maalampi, A. Pietila and M. Raidal, Nucl. Phys. **B487**, 27 (1997), [hep-ph/9606311].
[99] ATLAS Collaboration, ATLAS detector and physics performance. Technical design report. Vol. 2, CERN-LHCC-99-15.
[100] A. Ferrari and J. Collot, ATL-PHYS-2000-034.
[101] D. Benchekroun, C. Driouichi and A. Hoummada, Eur. Phys. J. direct **C3**, N3 (2001).
[102] E. Arik *et al.*, ATL-PHYS-2001-005.
[103] Particle Data Group, S. Eidelman *et al.*, Phys. Lett. **B592**, 1 (2004).
[104] R. N. Mohapatra, Phys. Rev. **D46**, 2990 (1992).
[105] V. M. Abazov *et al.* (D0 Collaboration), Phys. Rev. Lett. **93**, 141801 (2004), [hep-ex/0404015].
[106] D. Acosta *et al.* (CDF Collaboration), Phys. Rev. Lett. **93**, 221802 (2004), [hep-ex/0406073].
[107] M. L. Swartz, Phys. Rev. **D40**, 1521 (1989).
[108] D. Acosta *et al.* (CDF Collaboration), Phys. Rev. Lett. **95**, 071801 (2005), [hep-ex/0503004].
[109] T. Sjostrand *et al.*, Comput. Phys. Commun. **135**, 238 (2001), [hep-ph/0010017].
[110] E. Richter-Was, D. Froidevaux and L. Poggioli, ATL-PHYS-98-131.
[111] A. Pukhov *et al.*, hep-ph/9908288.
[112] F. Cuypers, hep-ph/9706255.